Huihui Bi, Sukanya Luang, Yuan Li, Natalia Bazanova, Nikolai Borisjuk, Maria Hrmova, Sergiy Lopato

Wheat drought-responsive WXPL transcription factors regulate cuticle biosynthesis genes

Plant Molecular Biology, 2017; 94(1):15-32

Wheat drought-responsive WXPL transcription factors regulate cuticle biosynthesis genes [S]

Huihui Bi, Sukanya Luang, Yuan Li, Natalia Bazanova, Nikolai Borisjuk[1], Maria Hrmova*, Sergiy Lopato

From The University of Adelaide, Waite Campus, Glen Osmond, South Australia 5064, Australia

[1] Current address: School of Life Science, Huaiyian Normal University, Huaian 223300, China

*To whom correspondence should be addressed; E-mail: maria.hrmova@adelaide.edu.au; Tel.: +61 8 8313 7160; Fax: +61 8 8313 7102.

[S] This article contains Figures 1-7, and Scheme 1, Tables 1-2, and Supporting Figures 1-2 and Supporting Tables 1-3.

The total word count of the manuscript is 9,086, including legend descriptions and excluding References.

Abbreviations: 3D, three-dimensional; ABA, abscisic acid; DOPE, discrete optimised protein energy; GFP, green fluorescent protein; HD-Zip IV, homeodomain-leucine zipper class IV; IWGSC, International Wheat Genome Sequencing Consortium; LEA, late embryogenesis abundant; MOF, modeller objective function; Q-PCR, quantitative PCR; Ta, *Triticum aestivum*; TF(s), transcription factor(s); WXP, WAX PRODUCTION; WXPL, WXP-like; Y1H, yeast-1-hybrid.

Keywords: Abiotic stress; Cuticle; DREB transcription factors; Drought; Molecular model; MYB transcription factors; Transcription factor networks.

GeneBank accession numbers: *TaWPXL1A* - KX611869; *TaWPXL1B* - KX611870; *TaWPXL1D* - KX611871; *TaWPXL2B* - KX611872; *TaWPXL2D* - KX611873.

Abstract

The cuticle forms a hydrophobic waxy layer that covers plant organs and provides protection from biotic and abiotic stresses. Transcription of genes responsible for cuticle formation is regulated by several types of transcription factors (TFs). Five orthologous to *WAX PRODUCTION* (*WXP1* and *WXP2*) genes from *Medicago truncatula* were isolated from a cDNA library prepared from flag leaves and spikes of drought tolerant wheat (*Triticum aestivum*, breeding line RAC875) and designated *TaWXP-like* (*TaWXPL*) genes. Tissue-specific and drought-responsive expression of *TaWXPL1D* and *TaWXPL2B* was investigated by quantitative RT-PCR in two Australian wheat genotypes, RAC875 and Kukri, with contrasting glaucousness and drought tolerance. Rapid dehydration and/or slowly developing cyclic drought induced specific expression patterns of *WXPL* genes in flag leaves of the two cultivars RAC875 and Kukri. TaWXPL1D and TaWXPL2B proteins acted as transcriptional activators in yeast and in wheat cell cultures, and conserved sequences in their activation domains were localised at their C-termini. The involvement of wheat WXPL TFs in regulation of cuticle biosynthesis was confirmed by transient expression in wheat cells, using the promoters of wheat genes encoding two cuticle biosynthetic enzymes, the 3-ketoacyl-CoA-synthetase and the cytochrome P450 monooxygenase. Using the yeast 1-hybrid (Y1H) assay we also demonstrated the differential binding preferences of TaWXPL1D and TaWXPL2B towards three stress-related DNA *cis*-elements. Protein structural determinants underlying binding selectivity were revealed using comparative 3D molecular modelling of AP2 domains in complex with *cis*-elements. A scheme is proposed, which links the roles of WXPL and cuticle-related MYB TFs in regulation of genes responsible for the synthesis of cuticle components.

Introduction

Environmental stresses, such as limited water supply, high salinity and extreme temperatures, impair significantly grain yields (Porter and Semenov 2005). Minimising yield losses associated with these challenges could be achieved by strategic research to increase understanding of the physiological and molecular mechanisms of plant responses to stresses, and by applying this understanding to the development of plants with improved stress tolerance (Hrmova and Lopato 2014; Reynolds et al. 2012).

Two Australian wheat genotypes, Kukri and RAC875, which deliver similar grain yields and quality in optimal growing environments, show a drastic yield difference under cyclic drought conditions typical for most wheat growing regions in Australia; the glaucous advanced breeding line, RAC875 out-yields glaucousless Kukri by 24%. These two genotypes have been subjected to intensive

physiological, genetic and metabolomics investigations, which have revealed a stronger ability of RAC875 to maintain tissue water potential under drought, associated with the glaucous surface coverage of RAC875 (Bennett et al. 2012a; Bennett et al. 2012b; Bowne et al. 2012; Izagloo et al. 2008). Our recent comparative studies on the morphological and biochemical properties of leaf cuticles of RAC875 and Kukri cultivars demonstrated that better drought tolerance of RAC875 correlates with a number of cuticle properties, such as shape and load of cuticle wax crystals, biochemical composition, cuticle thickness, and that some of these features are regulated by drought-responsive MYB TFs (Bi et al. 2016).

There is a range of experimental evidence demonstrating the involvement of a variety of TFs in regulation of cuticular wax biosynthesis, transport and accumulation (Beisson et al. 2003; Jetter and Kunst 2008; Jetter et al. 2006; Li-Beisson et al. 2010). Most of these TFs belong to one of three plant families: the APETALA2/ethylene-responsive factor (AP2/ERF) family, the myeloblastosis (MYB) family, or homeodomain-leucine zipper class IV (HD-Zip IV) factors (Borisjuk et al. 2014). Cuticle-related TFs were identified and characterised for their regulation of cuticle-associated genes in a number of plant species, including *Arabidopsis*, rice, barley, maize, *Medicago*, soybean, tomato and wheat (Bi et al. 2016; Borisjuk et al. 2014; Buxdorf et al. 2014; Giménez et al. 2015; La Rocca et al. 2015; Sela et al. 2013; Xu et al. 2016). Over-expression of several cuticle-related TFs altered cuticle deposition and/or composition, changed cuticle structure and permeability, and in many cases increased stress tolerance of transgenic plants (Aharoni et al. 2004; Javelle et al. 2010; Seo et al. 2011; Seo and Park 2011; Zhang et al. 2005, 2007).

The AP2/ERF superfamily, which is involved in regulation of plant development and responses to biotic and abiotic stresses (Elliott et al. 1996; Licausi et al. 2013), is one of the largest families of TFs in plants. It comprises AP2, ERF, Dehydration Responsive Element Binding (DREB) and Related to ABI3/VP1 (RAV) subfamilies, which were classified based on the number and sequence differences of AP2 domains and the presence of additional DNA binding domains (Mizoi et al. 2012). ERFs have a single AP2 domain, which usually binds an ethylene responsive *cis*-element, designated as a GCC-box (AGCCGCC) (Ecker 1995). In some cases, ERFs can also bind C-repeat elements (GACGCC), which are usually recognised by DREB proteins (Eini et al. 2013).
WAX PRODUCTION (WXP1 and WXP2) TFs from the legume *Medicago truncatula* are members of the AP2/ERF superfamily, and have been reported to participate in regulation of cuticle biosynthesis (Zhang et al. 2005, 2007). These TFs have a low level of protein sequence identity to members of the WIN1/SHN1 clade of the ERFs, which belong to a clade of intensively studied transcriptional regulators of cuticle biosynthesis and distribution (Aharoni et al. 2004; Buxdorf et al. 2014; Kannangara et al. 2007; Sela et al. 2013; Shi et al. 2011, 2013; Xu et al. 2016). Expression of

both *WXP* genes is abscisic acid (ABA)-dependent and controlled by drought, while *WXP1* is also strongly up-regulated by cold (Zhang et al. 2005).

Strong constitutive expression of *WXP1* in transgenic *Medicago sativa* (alfalfa) as well as expression of both *WXP1* and *WXP2* in transgenic *Arabidopsis* led to significantly increased cuticular wax deposition on plant leaves, which could be visually detected (Zhang et al. 2005, 2007). Metabolomics analysis of leaf cuticle composition of *WXP1* and *WXP2* transgenic *Arabidopsis* lines revealed several differences in contents and chain length distributions of various wax components. For example, the amount of n-alkanes, a major wax component of *Arabidopsis* leaves, increased in both *WXP1* and *WXP2* transgenic *Arabidopsis* compared to control plants. However, the content of primary alcohols increased in *WXP1* plants but decreased in *WXP2* plants. Changes were also detected in physical cuticle properties. A chlorophyll leaching assay showed no changes in leaf cuticle permeability of the *WXP1 Arabidopsis* plants but decreased permeability in *WXP1* transgenic alfalfa, while cuticle permeability of the *WXP2 Arabidopsis* plants was increased. Expression levels of three *FATTY SCID ELONGASE* (*FAE*)-like genes and two *LACERATA* (*LCR*, encoding cytochrome P450 monooxygenases) genes from the cuticle biosynthesis pathway were significantly higher in the *WXP1* transgenic alfalfa plants than in control plants (Zhang et al. 2005). Drought tolerance of all alfalfa and *Arabidopsis* transgenic *WXP* lines was considerably enhanced compared to control plants. By contrast, freezing tolerance improvement was observed only for the *WXP1* transgenic *Arabidopsis* lines, while the *WXP2* plants were more sensitive to low temperature than control wild type (WT) plants (Zhang et al. 2007). However, a direct connection between changes in cuticle properties and freezing tolerance were not demonstrated in the latter report. In addition, expression of *WXP1* in alfalfa and *WXP2* in *Arabidopsis* strongly interfered with growth and development of transgenic plants. No negative influence of *WXP1* expression occurred on the developmental phenotype of transgenic *Arabidopsis*, suggesting *WXP1* may be a promising candidate gene for engineering of drought and frost tolerance in some plant species (Zhang et al. 2005, 2007).

Several orthologues WXP proteins are described in the literature. Amongst them is RAP2.4 from *Arabidopsis* (Lin et al. 2008; Rae et al. 2011; Shaikhali et al. 2008). Initially RAP2.4 was found to be involved in mediating light and ethylene signalling (Lin et al. 2008), as it acts as redox-sensor and a transducer of redox information (Shaikhali et al. 2008). Expression of the *RAP2.4* gene was found to be down-regulated by light, but up-regulated by salt and drought stresses (Ferreira et al. 2013; Lin et al. 2008; Rae et al. 2011). Another WXP orthologue, *ZmDBF1*, is induced by ABA and drought and the product of this gene regulated the drought-inducible *ZmRab17* gene by direct binding to DRE (ACCGAC) *cis*-element in its promoter (Kizis and Pagès 2002). The soybean

GmDREB2 gene is responsive to ABA treatment, drought, high salinity, and low temperature. GmDREB2 activates expression of downstream genes in transgenic *Arabidopsis* by binding to DRE elements and increases free proline contents in transgenic tobacco (Chen et al. 2007). An orthologue of WXP2, BpDREB2 from the woody plant *Broussonetia papyrifera*, has three characteristic domains/motifs: AP2, a nuclear localisation signal and a C-terminal acidic activation domain. It specifically binds to a DRE sequence in the Y1H assay. The expression of *BpDREB2* gene is strongly induced by dehydration and high salinity. Constitutive expression of *BpDREB2* in transgenic *Arabidopsis* conferred tolerance to salt and freezing without causing growth retardation (Sun et al. 2014). A WXP2-like gene *GhDBP2*, encoding a DREB (A-6) subfamily protein, was isolated from seedlings of cotton (*Gossypium hirsutum*). *GhDBP2* transcripts were strongly induced in cotton cotyledons by ABA treatment, drought, high salinity, and low temperature. GhDBP2 bound a DRE *cis*-element in the promoter region of the stress-inducible Late Embryogenesis Activated (LEA) gene, *LEA D113*, and in transient expression assays in tobacco cells it activated reporter gene expression driven by the *LEA D113* promoter (Huang et al. 2008). Although involvement of MtWXP orthologues in drought response has been repeatedly demonstrated in a number of species, no data on their participation in regulation of the cuticle biosynthesis have been reported.

Recently, we have identified wheat drought-regulated TFs from the MYB family and characterised their involvement in regulation of cuticle biosynthesis (Bi et al. 2016). In this study we describe wheat homologues of WXP1 and WXP2, designated TaWXP-like (TaWXPL) TFs. The expression patterns of two *TaWXPL* genes were studied in different wheat tissues and in leaves of two wheat genotypes with contrasting drought tolerance under the conditions of rapid dehydration and under cyclic drought. Transactivation properties of TaWXPL1D and TaWXPL2B TFs were demonstrated in yeast and wheat cell culture, and positions of conserved activation domains (ADs) were localised. DNA-binding selectivity of WXPL proteins was demonstrated and structural determinants of AP2 domains underlining this specificity were revealed for both TFs using 3D molecular modelling. Involvement of TaWXPL1D and TaWXPL2B TFs in the control of cuticle biosynthesis was confirmed by demonstrating their ability to activate the promoters of cuticle biosynthesis-related genes in transient expression assays.

Materials and Methods

Plant material and cultivation

Plants of the wheat (*Triticum aestivum*) genotypes RAC875 and Kukri, previously described by Izanloo et al. (2008), were grown in a greenhouse in 112 x 76 x 50 cm containers, equipped with an

automatic watering system and continuous monitoring of soil water potential (Amalraj et al. 2015). For the cyclic drought experiment, drought-tolerant RAC875 and drought-sensitive Kukri were grown and cyclic drought treatment was applied (Supporting Fig. 1) as described by Harris et al. (2016).

Cloning of the wheat orthologues of WXP TFs

Protein sequences of MtWXP1 and MtWXP2 were retrieved from the National Centre for Biotechnology Information (NCBI, Bethesda, MD, USA), using accession numbers summarised by Borisjuk et al. (2014). To identify the closest wheat homologues, MtWXP sequences were used to search in NCBI and International Wheat Genome Sequencing Consortium (IWGSC) sequence databases linked to the Blast Portal at the Australian Centre for Plant Functional Genomics (ACPFG, University of Adelaide, Australia). The closest wheat genes to MtWXP1 and MtWXP2 were DREB responsive factor (DRF)-like genes, designated *DRFL1* and *DRFL2*. Five sequences (presumably protein products of homeologous genes) of these two groups were deposited in NCBI by other research group, but no functional characterisation of these genes has been reported. Six homeologues of *DRFL1* and *DRFL2* genes were found in the IWGSC databases. These were used to design homeologue-specific primers (Supporting Table S1) for gene amplification by nested PCR from cDNA pools prepared from leaves and spikes of the drought-tolerant wheat genotype RAC875 subjected to drought. PCR products were cloned into the pENTR/D-TOPO vector (Life Technologies, Victoria, Australia) as previously described (Bi et al. 2016). Protein sequence identity analyses of translated cDNAs (Table 1) were calculated using the Needleman-Wunsch algorithm (McWilliam et al. 2013).

Construction of the evolutionary relationships of proteins with single AP2-domain

To construct a phylogenetic tree of ERF and DREB factors (Fig. 1), we used 106 wheat sequences from the Plant Transcription Factor Database (Jin et al. 2014; http://planttfdb.cbi.pku.edu.cn), together with five wheat WXPL proteins (products of genes cloned in this study), two (WXP1 and WXP2) query proteins from the legume *Medicago truncatula* (Mt), and proteins with high protein sequence homology to WXP proteins from *Asparagus officinalis* (Ao), *Arabidopsis thaliana* (At), *Broussonetia papyrifera* (Bp), *Gossypium hirsutum* (Gh), *Glycine max* (Gm) and *Zea maize* (Zm). In the first instance, a total of 161 sequences were retrieved; 55 sequences were removed because they did not contain starting methionine. The names of previously published wheat ERFs and DREB TFs were used together with their accession numbers. The evolutionary history of representative ERF and DREB proteins was inferred using the Neighbor-Joining method (Saitou and Nei 1987).

Evolutionary distances were computed using the p-distance method (Nei and Kumar 2000) (with 1,000 bootstrap replications), and expressed in units of numbers of residue differences per site. All positions containing gaps and missing data were eliminated. Evolutionary analyses were conducted in MEGA6 (Tamura et al. 2013).

Gene expression analysis in different wheat tissues, under dehydration and cyclic drought

Gene expression of wheat *WXPL* genes was investigated in detached leaves, sampled at awn emergence stage subjected to rapid dehydration, and in plants subjected to cyclic drought as described by Bi et al. (2016). Quantitative RT-PCR (Q-PCR) analysis was performed on cDNA samples as described previously (Fletcher 2014) using gene specific primers listed in Supporting Table 1. Three of four wheat genes, encoding for actin, cyclophilin, elongation α factor and glyceraldehyde-3-phosphate dehydrogenase, were used for normalisation of expression (Fletcher 2014). Selection of the most appropriate three normalisation genes was based on pairwise comparisons among the four genes for each dataset. To analyse tissue specificity of gene expression, we also utilised a cDNA series prepared from different tissues of *T. aestivum* cv. Chinese Spring (Morran et al. 2011). Three biological and three technical replicates were used in all gene expression analysis experiments.

In-yeast activation assay and localisation of activation domains

Sets of full length and partial coding sequences (CDS) for *TaWPXL1D* were amplified by PCR with *Eco*RI and *Bam*HI restriction sites introduced in forward and reverse primers, respectively, and cloned in the same restriction sites of the pGBKT7 vector (Scientifix, Victoria, Australia). In the case of *TaWPXL2B*, *Nde*I and *Eco*RI restriction sites were used for cloning because a *Bam*HI site was found inside the CDS of *TaWPXL2B*. Each set included the full-length CDS, and versions with truncations at the 5' or 3' ends. All primer sequences are listed in Supporting Table 1. A transcriptional activation assay in yeast (*Saccharomyces cerevisiae*) was performed as described by Eini et al. (2013). Yeast transformants were first selected on synthetic defined (SD)/-Trp medium to prove that transformation of the pGBKT7 construct in yeast cells occurred. The yeast culture was replica-plated onto SD2 (-Trp, -His) medium containing 5 mM 3-Amino-1,2,4-Triazol (3AT). The ability of full-length or truncated wheat WPXL proteins to activate expression of the *HIS3* gene led to yeast growth on the selective medium.

Assessment of DNA-binding selectivity of WXPL TFs using a Y1H assay

The full length coding regions of *TaWXPL1D* and *TaWXPL2B* were amplified by PCR using the same pairs of primers as for the in-yeast activation assay, and cloned to the respective restriction sites of the pGADT7 vector (Supporting Table 1). Each of the resultant constructs was transformed into Y187 wild-type yeast (*S. cerevisiae*), and each of four strains derived from Y187 (yDRE, yCRT, yGCC and yHDZ1), that were prepared by integration of constructs containing tandem repeats of DRE, CRT, GCC-box and HDZ1 *cis*-elements, respectively. These repeats were inserted upstream of the yeast minimal promoter and the *HIS3* gene (Pyvovarenko and Lopato 2011). Yeast transformants carrying the plasmids were selected on SD/-Leu medium and replica-plated to SD2 (-Leu, -His) medium containing 10 mM 3AT. The ability of transformants to grow on the SD2 medium suggested an interaction of TaWXPL proteins with a respective *cis*-element. Y187 and yHDZ1 strains were used as negative controls. The rate of yeast growth observed for each of the evaluated *cis*-element/WXPL protein combination was reproducible in three technical replicates.

Domain boundary and post-translation modification analyses and sequence alignments

Domain boundary distributions were determined using SMART (Letunic et al. 2015). Sequence alignments between WXPL protein sequences were performed using Annotator (Gille et al. 2014) and ProMals3D (Pei et al. 2008). Predictions of post-translation modifications (phosphorylation, N-glycosylation, nuclear localisation motifs) were performed using the ExPASy Bioinformatics Resource Portal (Gasteiger et al. 2003).

Homology modelling of wheat WXPL1D and WXPL2B TFs

Structural models of wheat WXPL1D and WXPL2B, using the *Arabidopsis thaliana* protein AtERF1 in complex with the GCC-box (Protein Data Bank accession 1GCC) as a template (Allen et al. 1998), were generated through the MODELLER 9.16 (Sali and Blundell 1993). Nucleotide variations required in the DNA template from AtERF1 were introduced using Coot (Emsley et al. 2010). Fifty models of each WXPL were generated using the starting coordinates of AtERF1, and models with the lowest scores of the Modeller Objective Function (MOF) (Shen and Sali 2006), and Discrete Optimised Protein Energy (DOPE) (Eswar et al. 2008) were selected. These models were optimised through energy minimisation using FoldX (Schymkowitz et al. 2005). Final models were evaluated by ProSa2003 (Sippl 1993) and PROCHECK programs (Laskowski et al. 1993) to evaluate stereochemical quality and G-factors. Ramachandran statistics and G-factor (Laskowski et al. 1993), and ProSa2003 z-score (Sippl 1993) parameters are summarised in Supporting Table 2.

Assessment of promoter activation by WXPL TFs in a wheat transient expression assay

A transient expression assay was performed using *Triticum monoccocum* L. suspension cell culture, according to the procedure established by Eini et al. (2013). In this assay, cultivated wheat cells were co-bombarded with a vector expressing one of the wheat *WXPL* genes and a construct containing the β-glucuronidase reporter gene (*GUS*) fused to a promoter containing DREB, CBF and/or ERF binding sites. GUS expression from the WXPL-activated promoter was quantified 48 hours after bombardment. Promoters of three wheat cuticle biosynthesis-related genes: 3-ketoacyl CoA synthetase (*TaKCS1*; Acc. KU737579), cytochrome P450 monooxygenase (*TaATT1*; Acc. KU737578) and SHINE 1 TF (*TdSHN1*; Acc. KU737580), were cloned into the *GUS* expression vector pMDC164 and were used as targets for activation by WXPL TFs (Bi et al. 2016). Vectors for expression of WXPL proteins were constructed by recombinational cloning of *TaWXPL1D* and *TaWXPL2B* CDS into the pUbi vector (Bi et al. 2016). The pUbi-GFP construct was generated in a similar way and used as a negative control in all transient expression experiments. DREB and ERF specific *cis*-elements (DRE, CRT and GCC-box) in promoters were predicted using the Plant *Cis*-acting Regulatory DNA Elements database (PLACE, University of Pittsburgh, US) (Higo et al. 1999).

Statistical analyses of data

Statistical data analyses of gene expression levels under dehydration and cyclic drought were performed using two-way ANOVA with the Bonferroni test in GenStat 16th Edition (VSN International Ltd, Hemel Hempstead, UK). Genotype and time (Fig. 3) or treatment and time (Fig. 4) were used as sources of variation, and each gene was processed individually. For these analyses, we checked that homoscedastic variances were present. This was achieved by logarithmic transformation. The analysis of residual values employing individual treatment, showed that variance values improved and adopted nearly straight line profiles, as defined by Normal plot quantiles (by plotting residual values against the expected normal quantiles). This analysis indicated that the residuals were more normally distributed, and that our data of given sample sizes, could be processed as homoscedastic sets. Subsequently, we subjected numerical data to a two-way ANOVA analysis. Transient expression assay data were analysed using Student's t-tests.

Results

Gene cloning and the phylogenetic relationships of WXPL TFs with ERFs and DREB proteins

Five homeologues of two wheat *WXPL* genes, *WXPL1* and *WXPL2*, which may potentially be involved in regulation of cuticle biosynthesis under drought, were cloned by nested PCR from leaves

and spikes of the drought-tolerant wheat genotype RAC875. The protein sequences of two known cuticle regulators from *Medicago truncatula*, WXP1 and WXP2, were used to identify the closest wheat homologues as described in Materials and Methods. We intended to clone all three homeologues of each of these two wheat genes, but were able to clone only two homeologues of WXPL2. Details of the cloned wheat *WXPL* genes, including their names, accession numbers, protein sequence identities to MtWXP1 and MtWXP2, and chromosomal locations of respective genes are summarised in Table 1. Blast analysis of coding sequences of five wheat *WXPL* cDNAs using the IWGSC NRGene Assembly database linked to the Blast Portal, indicated that all *WXPL* genes are intron-less, and therefore cannot be regulated by alternative splicing. Investigation of the evolutionary relationships between 130 ERF/DREB members, including two WXPs from *Medicago truncatula* and products of the five cloned *WXPL* homeologues showed that TaWXPL1 homeologues grouped with MtWXP1, while TaWXPL2 homeologues grouped with MtWXP2 (Fig. 1A). Two wheat sequences from the Plant Transcription Factor Database (Tae043463 and Tae006260) also grouped within the MtWXP2 clade. These two sequences share 94.3% sequence identity and 96.1% sequence similarity, and are localised on chromosomes 4D and 4A, respectively; these locations were obtained by searching the IWGSC NRGene Assembly. Although these sequences differed from the WXPL1 and WXPL2 proteins, they exhibited high sequence conservation in the AP2 domains and C-terminal regions (Supporting Fig. 2). We have experimentally identified these C-terminal regions as activation domains (see below).

One wheat homeologue from each clade (TaWXPL1D and TaWXPL2B) was selected for further characterisation. When TaWXPL1D and TaWXPL2B were aligned using the Needleman-Wunsch algorithm (McWilliam et al. 2013) across 35 C-terminal residues, a high sequence identity (69% identity, 86% similarity) was noted in C-terminal domains (Fig. 1B). This may indicate that both proteins exhibit similar activation regions, and may have similar protein binding properties.

Expression of *WXPL* genes in wheat tissues

Expression of *TaWXPL1D* and *TaWXPL2B* was examined using Q-PCR in various tissues of *T. aestivum* cv Chinese spring (Fig. 2). The *TaWXPL1D* gene showed highest transcript levels in anthers and pistils before anthesis and moderate levels in leaves and other tested tissues. The expression pattern of *TaWXPL2B* gene had some similarity to that of its homologue, *TaWXPL1D*, but overall the levels of *TaWXPL2B* expression were low. The highest number of *TaWXPL2B* transcripts was observed in bracts, while lower levels of expression were found in pistils, anthers and leaves. In other tested tissues the transcript levels of *TaWXPL2B* were very low.

Influence of water deficit on expression of wheat *WXPL* genes

Expression of *TaWXPL1D* and *TaWXPL2B* was analysed by Q-PCR (i) in detached flag leaves of Kukri and RAC875 that were subjected to rapid dehydration, and (ii) in flag leaves of the same two cultivars growing under cyclic drought. The first experiment was designed to reveal rapid transient responses on dehydration. The second experiment focused on determining gene expression during long-lasting and repeatable cycles of drought.

Difference in glaucousness of flag leaves and peduncles of drought-sensitive Kukri and drought-tolerant RAC875 were observed (Fig. 3A), reflecting differences in content and structure of their epicuticular waxes (Bi et al. 2016).

During fast dehydration of flag leaves, the *TaWXPL1D* gene was rapidly upregulated in drought-tolerant RAC875, while in drought-sensitive Kukri upregulation was weak and statistically insignificant (Fig. 3B). Although the basal level of expression of this gene in flag leaves of Kukri was three-fold higher than the basal levels of expression in flag leaves of RAC875. In RAC875 a six-fold increase in a transcript number was observed after two hours of stress, and over the next five hours, transcript numbers continued to increase slowly (Fig. 3B, top-right panel).

Dehydration-induced changes in the expression of the *TaWXPL2B* gene also occurred differently in two wheat genotypes. The basal level of expression of *TaWXPL2B* in flag leaves of Kukri was about 1.6-fold higher than those in RAC875. In Kukri, the number of transcripts decreased rapidly by approximately 3.5-fold compared to the initial number of transcripts after two hours of dehydration; these levels remain the same during next five hours of dehydration. However, in RAC875, the number of transcripts decreased slightly during the first four hours of dehydration and after next three hours the number of transcripts returned to an initial level (Fig. 3B, bottom-right panel).

The induction of *TaWXPL1D* and *TaWXPL2B* expression by drought was further investigated in the flag leaves of wheat genotypes Kukri and RAC875 during three consecutive cycles of drought (Fig. 4). Flag leaf samples were collected at the beginning, in the middle and at the end of the first drought cycle, then at the end of the second drought cycle, and finally, a short time after the second re-watering (Bi et al. 2016; Supporting Fig. 1). No induction of the *TaWXPL1D* gene was observed in Kukri by drought. However, this gene was transiently up-regulated in RAC875 on the fifth day of the first drought cycle, while later the expression of this gene has promptly returned to its initial levels. By contrast, the *TaWXPL2B* gene in Kukri was activated by drought early and at the end of the first drought cycle the levels started to return to the initial levels of expression. These levels of expression remained the same at the end of the second drought cycle and short time after re-watering the expression of *TaWXPL2B* has returned to initial levels (Fig. 4, top-right panel). On the other

hand, the drought-inducible regulation of the *TaWXPL2B* gene in flag leaves of RAC875 was not observed.

Domain structure and the activation properties of WXPL TFs

Domain organisation of wheat WXPL proteins was investigated using the SMART protein domain analysis tool (Letunic et al. 2015). Each of wheat WXPL TFs was predicted to contain a single AP2 DNA-binding domain, localised approximately in the middle of proteins, and two (TaWXPL1) to five (TaWXPL2) low-complexity domains that were between eight to 58 residues long. Up to 38 Tyr and Ser phosphorylation sites were identified in the TaWXPL1 sequences following the AP2 domain, while in TaWXPL2 sequences, more than 50 Tyr and Ser phosphorylation sites were found, predominatly present in the N-terminal regions and before the AP2. At least three N-glycosylation sites were found in TaWXPL1 sequences; one site in the middle of the AP2 and two sites following the AP2 domain. In TaWXPL2 sequences, two N-glycosylation sites were identified, both of which preceded AP2. No nuclear localisation signals were predicted in WXPL sequences. AP2 domains exibited the features characteristic of DNA binding function, with a prevalance of positively charged arginine and lysine residues.

The presence and positions of activation domains (ADs) in wheat WXPL proteins were examined in yeast. Full-length and truncated *WXPL* genes at the 5' or 3' coding regions were fused to the sequence-encoding binding domain (BD) of yeast GAL4 TF. Constructs were used to transform yeast cells, and the presence of ADs in TFs was revealed as the ability of the yeasts to grow on a selective medium. Both full-length TaWXPL1D and TaWXPL2B proteins provided strong transcriptional activation of the yeast *HIS3* gene, the product of which supports yeast growth on selective medium deficient in histidine (Fig. 5A). Truncation D1 decreased the TaWXPL1D transactivation activity, and completely removed the ability of TaWXPL2B to activate the reporter gene. D2 truncations of TaWXPL1D and TaWXPL2B abolished the activation properties of both proteins, suggesting that significant portions of proteins responsible for transcriptional activation are located at the C-termini of WXPL proteins.

We also predicted the presence of transcriptional ADs in WXPL proteins, based on knowledge that ADs are usually (but not always) enriched in acidic amino acid residues and contain glutamine-rich and proline-rich motifs (Johnson et al. 1993). The alignment of 14 sequences, of the branch highlighted in blue lines in the phylogenetic tree in Fig. 1A, revealed the presence of a conserved motif/domain (Fig. 1B), characteristic of only WXPL TFs from wheat and other plants. The presence of several absolutely conserved hydrophobic and charged residues indicated that these domains may adopt a similar fold. We predicted (Scratch Protein Predictor; Cheng et al. 2005) that

this domain exhibits significant disorder, but carrying a C-terminal α-helix. A description of this C-terminal domain could not be found in ProDom (Bru et al. 2005) or SMART (Letunic et al. 2015) databases, although a 15-residue motif xFxLxKxPSxEIDWx was identified in the MEME suite (Bailey et al. 2009). We have termed this domain the 'Activation Domain of WXPL proteins' (AD-WXPL).

The DNA binding specificity of the TaWXPL1D and TaWXPL2B proteins

The DNA binding specificity of TaWXPL1D and TaWXPL2B was analysed using a Yeast 1-hybrid (Y1H) assay. Plasmids encoding GAL4 activation domain (AD) fusion proteins were used in the assay. The TaWXPL1D-GAL4 plasmids were transformed into yeast strain Y187 and each of four derivatives of this strain containing an integrated genomic DNA reporter gene under minimal yeast promoter with four repeats of one of the plant specific *cis*-elements DRE, CRT, GCC-box or HDZ1 (resultant strains were designated as yDRE, yCRT, yGCC and yHDZ1, respectively). Y187 and yHDZ strains were used as negative controls. The Y1H assay (Fig. 5B) revealed that both wheat WXPL proteins can recognise the *cis*-elements DRE, CRT and GCC-box, wich were earlier reported as elements specific for DREB TFs and/or ERFs (Baker et al. 1994; Ohme-Takagi and Shinshi 1995; Yamaguchi-Shinozaki and Shinozaki 1994). However, there were significant differences in the strength of protein-DNA binding between the two WXPL proteins. Interaction of TaWXPL1D with the CRT element was stronger than with the two other elements, which bound this protein with equally low eficiency. By contrast, TaWXPL2B showed very strong interaction with DRE, signigicantly weaker interaction with CRT and weak interaction with the GCC-box element (Fig. 5B).

Homology modelling of wheat WXPL1D and WXPL2B TFs

Domain boundaries analyses of wheat TaWXPL1D and TaWXPL2B proteins showed the presence of AP2 domains (with well-defined boundaries), and between two and five low-complexity domains. An alignment of the template (AtERF1) and the two wheat AP2 WXPL sequences (Fig. 6A) indicates that there is a high level of sequence identity between the investigated proteins. AP2 of the AtERF1 template shares 70% (with TaWXPL1D) and 75% (with TaWXPL2B), and 83% (with both TaWXPL proteins) sequence identity and similarity. The positions of ten identical residues and secondary structure element distributions between the template and target sequences indicate the presence of three β-sheets and one α-helix.

To understand variations in binding of the two wheat WXPL proteins with the DNA *cis*-elements CRT (5′-GCCGAC-3′/5'-GTCGGC-3'), DRE (5'-ACCGAC-3′/5'-GTCGGT-3') and GCC (5'-GCCGCC-3′/5'-GGCGGC-3'), we generated 3D models of AP2 domains of wheat TFs using AtERF1 as the template (PDB accession 1GCC in complex with the GCC box). The AP2 models of both WXPL proteins consist of a three-stranded anti-parallel β-sheet and an α-helix that is positioned almost in parallel to the β-sheet (Fig. 6B). The wheat WXPL proteins bound to the major groove of *cis*-elements *via* charge/polar (Arg, Glu, and Thr) and hydrophobic (Trp) residues in the three-stranded β-sheet, and *via* a Tyr residue from the α-helix. The Arg residue is predicted to bind the first bases of DNA sense strands (G_1 or A_1), while Thr and Trp always interact with the phosphate backbone (Fig. 6B, Supporting Table 3). However, in this model, the Arg residues of TaWXPL1D and TaWXPL2B interacted with first bases ($G_{1'}$) of antisense strands. The residues of TaWXPL1D and TaWXPL2B involved in interactions to CRT elements were found to be similar (Supporting Table 3), except that no interactions of Glu187 and Arg196 with the respective $C_{3'}$ and G_4 bases were found for TaWXPL2B. TaWXPL2B bound the DRE *cis*-element more specifically than CRT, because Arg179 not only contacted to the first base (A_1) in the sense strand, but also it interacted with its complementary base ($T_{6'}$) in the antisense strand. Moreover, Arg189 bonded to the A_5 base to increase the binding specificity. Investigation of interactions with the GCC *cis*-element revealed that the nucleobases of G_1, $G_{1'}$ and $C_{3'}$ made contacts to Arg115, Arg125 and Glu123 for TaWXPL1D, and to Arg179, Arg189 and Glu187 for TaWXPL2B, respectively. Additionally, TaWXPL1D formed hydrogen bonds to $G_{2'}$ and $G_{4'}$ of the GCC *cis*-element through Arg125 and Arg113, respectively, but these bonds were not found in the TaWXPL2B/GCC complex. It was notable that in the TaWXPL2a/GCC complex, Arg176 and Arg196 contacted G_4 or $G_{5'}$ bases, and hydrogen bond separations between residues and nucleobases or the sugar-phosphate backbone varied between 2.5 Å to 3.5 Å (Supporting Table 3).

Activation of promoters of cuticle biosynthesis-related genes by WXPL TFs

Three promoters of cuticle biosynthesis-related genes were cloned either by nested PCR using genomic DNA of *T. aestivum* as template (*TaATT1* and *TaKCS1* promoters), or *via* screening of a BAC library of *T. durum* (*TdSHN1* promoter) (Bi et al. 2016). Promoters were inserted upstream of the *GUS* reporter gene and resulting constructs were used in transient expression assays. These assays were conducted to confirm the involvement of wheat *WXPL* genes in regulation of cuticle biosynthesis. Transient expression assays were performed by co-bombardment of suspension cell culture of *T. monoccocum* L., with constructs containing the *GUS* gene driven by each of the tested

promoters (reporter constructs), and constructs containing each WXPL TF gene driven by the constitutive polyubiquitin promoter (effector constructs) (Fig. 7A). TaMYB74 (Bi et al. 2016) driven by polyubiquitin promoter was used as a positive control in the case of *TdSHN1* promoter activation. The *GFP* gene cloned under the polyubiquitin promoter was used as a negative control to reveal basal levels of promoter activity in wheat cells.

As shown in Fig. 7B, TaWXPL1D activated two promoters, *TaKCS1* and *TaATT1*, while TaWXPL2B activated only the *TaKCS1* promoter. Although the *TdSHN1* promoter was strongly activated by TaMYB74 (Bi et al. 2016), it was not activated by either of the wheat WXPL proteins (data not shown).

Discussion

The main function of cuticle, and of cuticular waxes in particular, is protection against excessive solar irradiation and conservation of internal plant water (Yeats and Rose 2013). Australian wheat cultivars, RAC875 (glaucous, drought tolerant) and Kukri (non-glaucous, drought sensitive), were previously characterised in terms of cuticle structure and composition as well as transcriptional regulation of cuticle biosynthesis by drought-regulated MYB TFs (Bi et al. 2016). Recently, we suggested that the main reason for the difference in leaf glaucousness between RAC875 and Kukri cultivars, is in the high content of β-diketones in the wax of RAC875 (Bi et al. 2016). In-line with our previous observations (Bi et al. 2016), β-diketones were proposed to be the major wax components responsible for the glaucous appearance of wheat and barley (Adamski et al. 2013; Zhang et al. 2013). Further, other researchers identified gene clusters responsible for accumulation of β-diketones in barley (Schneider et al. 2016) and wheat (Hen-Avivi et al. 2016) that in the latter case were localized in the *W1* locus of chromosome 2BS, which was previously shown to be the determinant for glaucousness. Although, to some extent, glaucousness and β-diketones play a role in drought tolerance of Australian wheat cultivars, other wax components such as alkanes, and changes in content of waxes inside the cutin layer might also play important roles in protection from dehydration during wheat growth under mild or cyclic drought.

In this work, two Australian wheat cultivars, RAC875 and Kukri were used with the aim to: (i) identify genes encoding wheat orthologues of WXP TFs that potentially may be involved in regulation of cuticular wax biosynthesis pathways under drought, (ii) functionally characterise wheat *WXP*-like genes and gene products, and (iii) to show the ability of wheat WXPL TFs to activate promoters of genes involved in cuticle biosynthesis.

Phylogenetic analysis of DREB/ERF proteins (Fig. 1) indicated that the five WXPL proteins cloned from the advanced breeding line RAC875 were grouped in two clades, together with WXP1 and WXP2 TFs from *Medicago truncatula* (Zhang et al. 2005, 2007). Alignments of protein sequences of wheat WXPL proteins (Supporting Fig. 2) revealed that the *TaWXPL1* cDNAs isolated from RAC875 are represented by all three homeologous genes (letters at the end of gene/protein names reflect their belonging to A, B or D genome of hexaploid wheat), while only two homeologues of *TaWXPL2* (B and D) were cloned. No significant differences in protein sequence were found between the homeologues which could potentially influence protein structure or function. Therefore, two representatives, *TaWXPL1D* and *TaWXPL2B*, one from each clade were selected for further characterisation.

It is notable, that the wheat genome contains a third type of *WXPL* genes (Tae043463 and Tae006260), which in our phylogenetic analysis grouped to the MtWXP2 clade, and which have a C-terminal activation domain similar to TaWXPL1 and TaWXPL2 (Fig. 1B). All WXPL homologues reported for different plant species grouping to the MtWXPL1 and MtWXP2 clades (Huang et al. 2008; Kizis and Pagès 2002; Lin et al. 2008; Liu et al. 2010; Rae et al. 2011; Shaikhali et al. 2008; Sun et al. 2014) are responsive to drought and some other abiotic stresses.

The analysis of gene activity in different tissues of wheat plants grown under optimal well-watered conditions, revealed both similarities and differences in the expression patterns of *TaWXPL1D* and *TaWXPL2B* (Fig. 2). There were relatively high levels of *TaWXPL1D* gene expression in all tested tissues, in contrast to a more tissue-specific pattern of TaWXPL2B. This may suggest a broad involvement of the product of *TaWXPL1D* in regulation of biochemical and physiological processes in wheat. By contrast, TaWXPL2B in the absence of stress may participate mostly in gene regulation in specific wheat tissues. Notable differences in levels of expression of *TaWXPL1D* and *TaWXPL2B* were observed in bracts. The highest expression levels of both genes were found in flowers.

Transcripts of both *WXP* genes from legume *Medicago truncatula* (Zhang et al. 2005, 2007), *RAP2.4* from *Arabidopsis* (Lin et al. 2008), *ZmDBF1* from maize (Kizis and Pagès 2002), *GmDREB2* from soybean (Chen et al. 2007), and other *WXP* homologues were reported to be up-regulated by ABA and abiotic stresses. We have compared expression of wheat WXPL genes under two different regimes of dehydration in two wheat genotypes with contrast drought tolerance. The impact on TF genes during stress is often rapid and transient: after some time the levels of transcripts return to initial levels, even if the stress factor is persisting. Therefore, changes in expression of TF genes with a short transient response are sometimes difficult to detect if the stress, e.g. drought, develops slowly. For these reasons we used two regimes of low water stress: rapid dehydration and

slowly developing cyclic drought (Bi et al. 2016). The aim of the first experiment was to detect rapid and transient changes in expression of *WXPL* genes. The aim of the second experiment was to detect long-lasting and late-occurring changes in expression levels of *WXPL* genes under the conditions of two successive cycles of drought.

We found that both wheat *WXPL* genes are regulated by dehydration and drought. Similarly to drought-regulated cuticle-related *MYB* genes (Bi et al. 2016), reasonable correlation was observed for wheat *WXPL* genes for expression patterns under two regimes of dehydration in both Kukri and RAC875, with the exception of *TaWXPL2B* in Kukri. The *TaWXPL2B* gene in Kukri was clearly downregulated by rapid dehydration and transiently upregulated in the first cycle of drought, but was not significantly affected in RAC875 under the same dehydration regimes. Such behaviour may suggest that *TaWXPL2B* is regulated differently by different components of drought, and that expression of this gene depends on a component that prevails during a particular type or time of stress. *TaWXPL2B* may be an early-activated type of a regulatory gene, which is initially triggered by elevated ABA levels and other factors, under the conditions of a low level of dehydration, but later downregulated by increasing dehydration of drought-sensitive plants, *e.g.* by osmotic stress. The RAC875 cultivar is much better protected against drought, particularly the dehydration component, than Kukri. This characteristic was recently demonstrated by water-loss and chlorophyll-leaching tests (Bi et al. unpublished data). Therefore, the drought-responsive regulation of *TaWXPL2B* expression in RAC875 might not be required for the acquisition of drought tolerance.

The patterns of expression of *TaWXPL2B* and *TaMYB24* (Bi et al. 2016) are surprisingly similar in both studied wheat cultivars, suggesting their cooperation in activation of the same gene pools during dehydration.

The *TaWXPL1D* gene was not affected by either rapid dehydration or cyclic drought in the drought sensitive Kukri, but it was clearly upregulated under both stress regimes in the drought tolerant RAC875. This suggests a potential role of this gene in the development of high drought tolerance of RAC875. *TaWXPL1D* may be an exciting candidate for engineering of enhanced drought tolerance. It would be interesting to overexpress this gene in Kukri or another drought-sensitive wheat genotype under a moderate constitutive or drought-responsive promoter, and to compare stress tolerance of the generated transgenic lines with stress tolerance of wild type plants.

As previously reported, the *Arabidopsis* orthologue of TaWXPL2 proteins, RAP2.4, can bind to different stress-responsive elements in gene promoters, including the ethylene-responsive GCC-box, dehydration-responsive element (DRE) (Lin et al. 2008) and the CGCG core of a CE3-like element (Shaikhali et al. 2008). Using a Y1H assay we have demonstrated that both WXPL proteins can bind to each of three tested *cis*-elements specific for ERFs and/or DREB TFs, but that they show

obvious sequence binding preferences. The TaWXPL1D protein demonstrated higher affinity for the CRT (GCCGAC) element compared to two other *cis*-elements, DRE (ACCGAC) and GCC-box (GCCGCC), which this protein bound with similar low efficiency (Fig. 5A). By contrast, TaWXPL2B clearly preferred DRE to other tested elements, interacted less efficiently with CRT and even less efficiently with the GCC-box. Small differences in protein sequences were found between the AP2 domains of TaWXPL1D and TaWXPL2B, which are sufficient to provide different DNA-binding specificity and hence activation of diverse groups of target genes. Analysis of molecular models of protein-DNA interactions revealed possible bases of different binding strengths. To understand why TaWXPL1D better binds CRT (GCCGAC) and TaWXPL2B stronger binds DRE (ACCGAC), one should consider that a total of 13 and 14 respective hydrogen bonds to nucleobases are formed in protein-DNA complexes. In other words, there are different hydrogen bond distributions in both complexes; it has been estimated that a loss of one hydrogen bond corresponds to approximately 1 kcal/mol (Fersht 1987). In the TaWXPL2B/DRE complex two unique hydrogen bonds are formed to nucleobases, while in the TaWXPL1D/CRT complex, one less hydrogen bond is present and simultaneously Arg125 forms two nearly identical hydrogen bonds to the antisense DNA strand (Supporting Table 3). Notably, no differences in the number of DNA phospho-diester backbone bonds were found between the two protein complexes.

Wheat WXPL proteins act as transcriptional activators. The C-terminal activation domains, designated here as AD-WXPL, were initially identified at the C-termini of all analysed WXP-like proteins (including representatives from other plants) as conserved sequences (Sun et al., 2014). The proposed function of AD-WXPLs as activation domains was confirmed in in-yeast activation assays using truncated versions of TaWXPL1D and TaWXPL2B proteins (Fig. 5A).

A transient expression assay in wheat suspension cells was used to confirm the participation of drought-affected wheat WXPL TFs in transciptional activation of cuticle-related genes (Fig. 7). For these purposes the closest wheat homologues of the *Arabidopsis ATT1* gene, encoding an enzyme from the cutin biosynthetic pathway, the *KCS1* gene, encoding an enzyme from the wax biosynthetic pathway, and *WIN1*/*SHN1* encoding the regulator of wax biosynthesis were used as the representative genes of corresponding pathways. *TaATT1*, *TaKCS1* and *TdSHN1* promoters (Bi et al. 2016) were tested in this work as the promoters of potential target genes of wheat WXPL TFs. In our assay, the TaWXPL1D protein activated two (*TaATT1* and *TaKCS1*) promoters, and TaWXPL2B protein activated one (*TaKCS1*) promoter, and therefore both TFs may be considered as good candidates for cuticle biosynthesis-related regulators in wheat. Neither WXPL TFs activated the *TdSHN1* promoter. Hence, the WXPL TFs demonstrated selectivity in target gene activation and can

potentially collaborate with cuticle biosynthesis-related MYB TFs during activation of the *TaATT1* and *TaKCS1* promoters.

The results of promoter activation in wheat cells are in a good agreement with the results of DNA binding selectivity obtained in the Y1H assay. *In silico* analysis of the promoter sequences of *TaATT1*, *TaKCS1* and *TdSHN1* (including 5'-UTRs) identified different representations of CRT, DRE and GCC-box elements (Table 2). It is plausible that TaWXPL2B, which demonstrated the highest affinity for DRE in the Y1H assay, requires this specific element for promoter activation, as it activated the *TaKCS1* promoter containing two DRE elements but did not activate the *TaATT1* promoter, which has no DRE elements. By contrast, TaWXPL1D showed highest affinity for CRT in the Y1H assay, and activated both *TaATT1* and *TaKCS1* promoters, which have four and two CRT elements, respectively. Inability of either of wheat WXPL TFs to activate the *TdSHN1* promoter is a logical consequence of the absence of the corresponding *cis*-elements. A single DRE of this promoter might be inactive because of its position or adjacent sequences; alternatively, the activation through these elements requires cooperation of DREB/ERF with other TFs/co-factors, which may be essential for a strong binding and/or activation of the *TdSHN1* promoter.

The transient expression assay we used for confirmation and analysis of wheat cuticle-related TFs is relatively robust, rapid and reliable. The use of a wheat cell suspension culture for transient expression is a good option for the preliminary confirmation of regulatory effects of TFs on particular promoters, and also provides a convenient method for verification of DNA constructs for stable gene overexpression or for component delivery in emerging genome editing technologies (Baltes and Voytas 2015). This approach provides several other advantages, including the possibility to test promoter activation by two or more TFs simultaneously and to identify functional *cis*-elements on promoters (Bi et al. 2016; Eini et al. 2013).

Scheme 1 is an extended version of an earlier published scheme (Bi et al. 2016). It summarises our findings of the activation of cuticle biosynthetic pathways in wheat by drought-inducible TFs TaWXPL1, TaWXPL2, TaMYB31 and TaMYB74, homologues of the well-characterised cuticle biosynthesis regulators MtWXP1 and MtWXP2 (Zhang et al. 2005, 2007), AtMYB96 (Seo et al. 2011) and AtMYB41 (Cominelli et al. 2008). Expression of all four wheat TFs was upregulated by drought and/or dehydration, and three of them activated both *ATT1* and *KCS1* genes through direct binding to their promoters, albeit with different efficiencies (Bi et al. 2016). Further experiments and particularly the generation of transgenic wheat plants will be required to elucidate cooperative regulation of the *TaATT1* and *TaKCS1* promoters by WXPL and MYB TFs and confirm the roles of these TFs in cuticle biosynthesis.

In conclusion, differences in expression patterns of *TaWXPL2B* and *TaWXPL1D* under dehydration together with variances in DNA binding selectivity of the corresponding proteins to stress-related *cis*-elements suggest the possible involvement of wheat WXPL TFs in regulation of different sets of stress-responsive genes, including genes related to cuticle biosynthesis under stress, although some overlap in function may exist. Transient expression assay data, demonstrating activation of the *TaKCS1* promoter by both WXPL TFs but activation of the *TaATT1* promoter only by TaWXPL1D, strongly support this hypothesis. Characterisation of WXP homologues in other plant species suggests that in addition to regulating cuticle amount and quality, wheat WXPL TFs could also confer drought tolerance through different pathways, *e.g.* through the modulation of water homeostasis by downregulation of aquaporin genes (Rae et al. 2011) or by increasing free proline content (Chen et al. 2007). Further research should be aimed at investigation of other WXPL roles in wheat.

Acknowledgments

We thank Dr Julie Hayes for critically reading the manuscript, Mr Paul Eckermann for advice on the mathematical treatment of data, and anonymous reviewers for constructive suggestions on the manuscript. The China Scholarship Council and the University of Adelaide are acknowledged for providing HB a joint postgraduate scholarship. This work was supported by the Australian Centre for Plant Functional Genomics, and by the Australian Research Council (to MH and SLo), the Grains Research & Development Corporation and the Government of South Australia.

Author contributions statement: HB performed most of the experiments. NB and YL assisted with experiments. SLu and MH performed molecular modelling. SLo, NBo and MH guided research and wrote the manuscript.

Compliance with ethical standards: Conflict of interest Authors declare that they have no conflict of interest.

References

Adamski NM, Bush MS, Simmonds J, Turner AS, Mugford SG, Jones A, Findlay K, Pedentchouk N, von Wettstein-Knowles P, Uauy C (2013) The inhibitor of *wax 1* locus (*Iw1*) prevents

formation of β- and OH-β-diketones in wheat cuticular waxes and maps to a sub-cM interval on chromosome arm 2BS. Plant J 74:989-1002

Aharoni A, Dixit S, Jetter R, Thoenes E, van Arkel G, Pereira A (2004) The SHINE clade of AP2 domain transcription factors activates wax biosynthesis, alters cuticle properties, and confers drought tolerance when overexpressed in *Arabidopsis*. Plant Cell 16:2463-2480

Allen MD, Yamasaki K, Ohme-Takagi M, Tateno M, Suzuki M (1998) A novel mode of DNA recognition by a beta-sheet revealed by the solution structure of the GCC-box binding domain in complex with DNA. EMBO J 17:5484-5496

Amalraj A, Luang S, Kumar MY, Sornaraj P, Eini O, Kovalchuk N, Bazanova N, Li Y, Yang N, Eliby S, Langridge P, Hrmova M, Lopato S (2016) Change of function of the wheat stress-responsive transcriptional repressor TaRAP2.1L by repressor motif modification. Plant Biotechnol J 14:820-832

Bailey TL, Bodén M, Buske FA, Frith M, Grant CE, Clementi L, Ren J, LI WW, Noble WS (2009) MEME SUITE: tools for motif discovery and searching. Nucleic Acids Res 37:W202-W208

Baker SS, Wilhelm KS, Thomashow MF (1994) The 5′-region of *Arabidopsis thaliana cor15a* has *cis*-acting elements that confer cold-, drought-and ABA-regulated gene expression. Plant Mol Biol 24:701-713

Baltes NJ, Voytas DF (2015) Enabling plant synthetic biology through genome engineering. Trends Biotechnol 33:120-131

Beisson F, Koo AJ, Ruuska S, Schwender J, Pollard M, Thelen JJ, Paddock T, Salas JJ, Savage L, Milcamps A, Mhaske VB, Cho Y, Ohlrogge JB (2003) *Arabidopsis* genes involved in acyl lipid metabolism. A 2003 census of the candidates, a study of the distribution of expressed sequence tags in organs, and a web-based database. Plant Physiol 132:681-697

Bennett D, Izanloo A, Reynolds M, Kuchel H, Langridge P, Schnurbusch T (2012a) Genetic dissection of grain yield and physical grain quality in bread wheat (*Triticum aestivum* L.) under water-limited environments. Theor Appl Genet 125:255-271

Bennett D, Izanloo A, Edwards J, Kuchel H, Chalmers K, Tester M, Reynolds M, Schnurbusch T, Langridge P (2012b) Identification of novel quantitative trait loci for days to ear emergence and flag leaf glaucousness in a bread wheat (*Triticum aestivum* L.) population adapted to southern Australian conditions. Theor Appl Genet 124:697-711

Bi H, Luang S, Li Y, Bazanova N, Morran S, Song Z, Perera MA, Hrmova M, Borisjuk N, Lopato S Identification and characterization of wheat drought-responsive MYB transcription factors involved in the regulation of cuticle biosynthesis. J Exp Bot, doi:10.1093/jxb/erw298

Borisjuk N, Hrmova M, Lopato S (2014) Transcriptional regulation of cuticle biosynthesis. Biotechnol Adv 32:526-540

Bowne JB, Erwin TA, Juttner J, Schnurbusch T, Langridge P, Bacic A, Roessner U (2012) Drought responses of leaf tissues from wheat cultivars of differing drought tolerance at the metabolite level. Mol Plant 5:418-429

Bru C, Courcelle E, Carrère S, Beausse Y, Dalmar S, Kahn D (2005) The ProDom database of protein domain families: more emphasis on 3D. Nucleic Acids Res 33:D212-D215

Buxdorf K, Rubinsky G, Barda O, Burdman S, Aharoni A, Levy M (2014) The transcription factor SlSHINE3 modulates defense responses in tomato plants. Plant Mol Biol 84:37-47

Chen M, Wang QY, Cheng XG, Xu ZS, Li LC, Ye XG, Xia LQ, Ma YZ (2007) GmDREB2, a soybean DRE-binding transcription factor, conferred drought and high-salt tolerance in transgenic plants. Biochem Biophys Res Commun 353:299-305

Cheng J, Randall A, Sweredoski M, Baldi P (2005) SCRATCH: A protein structure and structural feature prediction server. Nucleic Acids Res 33:W72-W76

Cominelli E, Sala T, Calvi D, Gusmaroli G, Tonelli C (2008) Over-expression of the Arabidopsis *AtMYB41* gene alters cell expansion and leaf surface permeability. Plant J 53:53-64

Cui F, Brosché M, Lehtonen MT, Amiryousefi A, Xu E, Punkkinen M, Valkonen JP, Fujii H, Overmyer K (2016) Dissecting abscisic acid signaling pathways involved in cuticle formation. Mol Plant 9:926-938

Ecker JR (1995) The ethylene signal transduction pathway in plants. Science 268:667-675

Eini O, Yang N, Pyvovarenko T, Pillman K, Bazanova N, Tikhomirov N, Eliby S, Shirley N, Sivasankar S, Tingey S, Langridge P, Hrmova M, Lopato S (2013) Complex regulation by Apetala2 domain-containing transcription factors revealed through analysis of the stress-responsive *TdCor410b* promoter from durum wheat. PloS One 8:e58713

Elliott RC, Betzner AS, Huttner E, Oakes MP, Tucker WQ, Gerentes D, Perez P, Smyth DR (1996) *AINTEGUMENTA*, an *APETALA2*-like gene of *Arabidopsis* with pleiotropic roles in ovule development and floral organ growth. Plant Cell 8:155-168

Emsley P, Lohkamp B, Scott WG, Cowtan K (2010) Features and development of Coot. Acta Crystallogr D66:486-501

Eswar N, Eramian D, Webb B, Shen MY, Sali A (2008) Protein structure modeling with MODELLER. Methods Mol Biol 426:145-159

Ferreira Neto JR, Pandolfi V, Guimaraes FC, Benko-Iseppon AM, Romero C, Silva RL, Rodrigues FA, Abdelnoor RV, Nepomuceno AL, Kido EA (2013) Early transcriptional response of soybean contrasting accessions to root dehydration. PLoS One 8:e83466

Fersht AR (1987) The hydrogen bond in molecular recognition. Trends Biochem Sci 12:301-304

Fletcher SJ (2014) qPCR for quantification of transgene expression and determination of transgene copy number. Methods Mol Biol 1145:213-237

Gasteiger E, Gattiker A, Hoogland C, Ivanyi I, Appel RD, Bairoch A (2003) ExPASy: the proteomics server for in-depth protein knowledge and analysis. Nucleic Acids Res 31:3784-3788

Gille C, Fähling M, Wey B, Wiel T, Gille A (2014) Alignment-annotator web server: rendering and annotating sequence alignments. Nucleic Acids Res 42:W3-W6

Giménez E, Dominguez E, Pineda B, Heredia A, Moreno V, Lozano R, Angosto T (2015) Transcriptional activity of the MADS box *ARLEQUIN*/*TOMATO AGAMOUS-LIKE1* gene is required for cuticle development of tomato fruit. Plant Physiol 168:1036-1048

Harris JC, Sornaraj P, Taylor M, Bazanova N, Baumann U, Lovell B, Langridge P, Lopato S, Hrmova M (2016) Molecular interactions of the gamma-clade homeodomain-leucine zipper class I transcription factors during the wheat response to water deficit. Plant Mol Biol 90:435-452

Hen-Avivi S, Savin O, Racovita RC, Lee WS, Adamski NM, Malitsky S, Almekias-Siegl E, Levy M, Vautrin S, Bergès H, Friedlander G, Kartvelishvily E, Ben-Zvi G, Alkan N, Uauy C, Kanyuka K, Jetter R, Distelfeld A, Aharoni A (2016) A metabolic gene cluster in the wheat *W1* and the barley *Cer-cqu* loci determines β-diketone biosynthesis and glaucousness. Plant Cell 28:1440-1460

Higo K, Ugawa Y, Iwamoto M, Korenaga T (1999) Plant *cis*-acting regulatory DNA elements (PLACE) database: 1999. Nucleic Acids Res 27:297-300

Hrmova M, Lopato S (2014) Enhancing abiotic stress tolerance in plants by modulating properties of stress responsive transcription factors. In: Genomics of Plant Genetic Resources (Tuberosa R, Graner A, Frison E, eds.), Springer Netherlands, 515 pp, Volume 2, Part II: Crop productivity, food security and nutritional quality, pp 291-316

Huang B, Jin L, Liu JY (2007) Identification and characterization of the novel gene *GhDBP2* encoding a DRE-binding protein from cotton (*Gossypium hirsutum*). J Plant Physiol 165:214-223

Javelle M, Vernoud V, Depege-Fargeix N, Arnould C, Oursel D, Domergue F, Sarda X, Rogowsky PM (2010) Overexpression of the epidermis-specific homeodomain-leucine zipper IV transcription factor Outer Cell Layer1 in maize identifies target genes involved in lipid metabolism and cuticle biosynthesis. Plant Physiol 154:273-286

Jetter R, Kunst L (2008) Plant surface lipid biosynthetic pathways and their utility for metabolic engineering of waxes and hydrocarbon biofuels. Plant J 54:670-683

Jetter R, Kunst L, Samuels AL (2006) Composition of plant cuticular waxes. Blackwell Publishing, Oxford

Jin J, Zhang H, Kong L, Gao G, Luo J (2014) PlantTFDB 3.0: a portal for the functional and evolutionary study of plant transcription factors. Nucleic Acids Res 42: D1182-7

Johnson PF, Sterneck E, Williams SC (1993) Activation domains of transcriptional regulatory proteins. J Nutr Biochem 4:386-398

Kannangara R, Branigan C, Liu Y, Penfield T, Rao V, Mouille G, Höfte H, Pauly M, Riechmann JL, Broun P (2007) The transcription factor WIN1/SHN1 regulates Cutin biosynthesis in *Arabidopsis thaliana*. Plant Cell 19:1278-1294

Kizis D, Pagès M (2002) Maize DRE-binding proteins DBF1 and DBF2 are involved in *rab17* regulation through the drought-responsive element in an ABA-dependent pathway. Plant J 30:679-89

La Rocca N, Manzotti PS, Cavaiuolo M, Barbante A, Dalla Vecchia F, Gabotti D, Gendrot G, Horner DS, Krstajic J, Persico M, Rascio N, Rogowsky P, Scarafoni A, Consonni G (2015) The maize *fused leaves1* (*fdl1*) gene controls organ separation in the embryo and seedling shoot and promotes coleoptile opening. J Exp Bot 66:5753-5767

Laskowski RA, Macarthur MW, Moss DS, Thornton JM (1993) PROCHECK: a program to check the stereochemical quality of protein structures. J Appl Crystall 26:283-291

Letunic I, Doerks T, Bork P (2015) SMART: recent updates, new developments and status in 2015. Nucleic Acids Res 43:D257-260

Li-Beisson Y, Shorrosh B, Beisson F, Andersson MX, Arondel V, Bates PD, Baud S, Bird D, Debono A, Durrett TP, Franke RB, Graham IA, Katayama K, Kelly AA, Larson T, Markham JE, Miquel M, Molina I, Nishida I, Rowland O, Samuels L, Schmid KM, Wada H, Welti R, Xu C, Zallot R, Ohlrogge J (2010) Acyl-lipid metabolism. The Arabidopsis book / American Society of Plant Biologists 8:e0133

Licausi F, Ohme-Takagi M, Perata P (2013) APETALA2/Ethylene Responsive Factor (AP2/ERF) transcription factors: mediators of stress responses and developmental programs. New Phytol 199:639-649

Lin RC, Park HJ, Wang HY (2008) Role of *Arabidopsis* RAP2.4 in regulating light- and ethylene-mediated developmental processes and drought stress tolerance. Mol Plant 1:42-57

Liu Y, Chen H, Zhuang D, Jiang D, Liu J, Wu G, Yang M, Shen S (2010) Characterization of a DRE-binding transcription factor from Asparagus (*Asparagus officinalis* L.) and its overexpression in *Arabidopsis* resulting in salt-and drought-resistant transgenic plants. Int J Plant Sci 171:12-23

Mizoi J, Shinozaki K, Yamaguchi-Shinozaki K (2012) AP2/ERF family transcription factors in plant abiotic stress responses. Biochim Biophys Acta 1819:86-96

Morran S, Eini O, Pyvovarenko T, Parent B, Singh R, Ismagul A, Eliby S, Shirley N, Langridge P, Lopato S (2011) Improvement of stress tolerance of wheat and barley by modulation of expression of DREB/CBF factors. Plant Biotechnol J 9:230-249

Nei M, Kumar S (2000) Molecular Evolution and Phylogenetics. Oxford University Press Inc, New York, NY

Ohme-Takagi M, Shinshi H (1995) Ethylene-inducible DNA binding proteins that interact with an ethylene-responsive element. Plant Cell 7:173-182

Porter J, Semenov M (2005) Crop responses to climatic variation. Philos Trans R Soc Biol Sci 360:2021–2035

Pei JM, Tang M, Grishin NV (2008) PROMALS3D web server for accurate multiple protein sequence and structure alignments. Nucleic Acids Res 36:W30–W34

Pyvovarenko T, Lopato S (2011) Isolation of plant transcription factors using a yeast one-hybrid system. Methods Mol Biol 754:45-66

Rae L, Lao NT, Kavanagh TA (2011) Regulation of multiple aquaporin genes in Arabidopsis by a pair of recently duplicated DREB transcription factors. Planta. 234:429-444

Reynolds M, Foulkes J, Furbank R, Griffiths S, King J, Murchie E, Parry M, Slafer G (2012) Achieving yield gains in wheat. Plant Cell Env 35:1799-1823

Saitou N, Nei M (1987) The neighbor-joining method: a new method for reconstructing phylogenetic trees. Mol Biol Evol 4:406-425

Sali A, Blundell TL (1993) Comparative protein modelling by satisfaction of spatial restraints. J Mol Boil 234: 779-815

Schymkowitz JW, Rousseau F, Martins IC, Ferkinghoff-Borg J, Stricher F, Serrano L (2005) Prediction of water and metal binding sites and their affinities by using the Fold-X force field. Proceed Natl Acad Sci USA 102:10147-10152

Shen MY, Sali A. (2006) Statistical potential for assessment and prediction of protein structures. Protein Sci 15:2507-2524

Sela D, Buxdorf K, Shi JX, Feldmesser E, Schreiber L, Aharoni A, Levy M (2013) Overexpression of AtSHN1/WIN1 provokes unique defense responses. PLoS One 8:e70146

Seo PJ, Lee SB, Suh MC, Park MJ, Go YS, Park CM (2011) The MYB96 transcription factor regulates cuticular wax biosynthesis under drought conditions in Arabidopsis. Plant Cell 23:1138-1152

Seo PJ, Park CM (2011) Cuticular wax biosynthesis as a way of inducing drought resistance. Plant Signal Behav 6:1043-1045

Shaikhali J, Heiber I, Seidel T, Ströher E, Hiltscher H, Birkmann S, Dietz KJ, Baier M (2008) The redox-sensitive transcription factor Rap2.4a controls nuclear expression of 2-Cys peroxiredoxin A and other chloroplast antioxidant enzymes. BMC Plant Biol 8:48

Shi JX, Adato A, Alkan N, He Y, Lashbrooke J, Matas AJ, Meir S, Malitsky S, Isaacson T, Prusky D, Leshkowitz D, Schreiber L, Granell AR, Widemann E, Grausem B, Pinot F, Rose JK, Rogachev I, Rothan C, Aharoni A (2013) The tomato SlSHINE3 transcription factor regulates fruit cuticle formation and epidermal patterning. New Phytol 197: 468-480

Shi JX, Malitsky S, De Oliveira S, Branigan C, Franke RB, Schreiber L, Aharoni A (2011) SHINE transcription factors act redundantly to pattern the archetypal surface of Arabidopsis flower organs. PLoS Genet 7:e1001388

Schneider LM, Adamski NM, Christensen CE, Stuart DB, Vautrin S, Hansson M, Uauy C, von Wettstein-Knowles P (2016) The *Cer-cqu* gene cluster determines three key players in a β-diketone synthase polyketide pathway synthesizing aliphatics in epicuticular waxes. J Exp Bot, doi: 10.1093/jxb/erw105

Sippl MJ (1993) Recognition of errors in three-dimensional structures of proteins. Proteins 17:355-362

Sun J, Peng X, Fan W, Tang M, Liu J, Shen S (2014) Functional analysis of *BpDREB2* gene involved in salt and drought response from a woody plant *Broussonetia papyrifera*. Gene 535:140-149

Tamura K, Stecher G, Peterson D, Filipski A, Kumar S (2013) MEGA6: Molecular Evolutionary Genetics Analysis version 6.0. Mol Biol Evol 30:2725-2729

McWilliam H, Li W, Uludag M, Squizzato S, Park YM, Buso N, Cowley AP, Lopez R (2013) Analysis tool web services from the EMBL-EBI. Nucleic Acids Res 41:W597-600

Xu Y, Wu H, Zhao M, Wu W, Xu Y, Gu D (2016) Overexpression of the transcription factors GmSHN1 and GmSHN9 differentially regulates wax and cutin biosynthesis, alters cuticle properties, and changes leaf phenotypes in *Arabidopsis*. Int J Mol Sci 17, pii: E587. doi: 10.3390/ijms17040587

Yamaguchi-Shinozaki K, Shinozaki K (1994) A novel *cis*-acting element in an *Arabidopsis* gene is involved in responsiveness to drought, low-temperature, or high-salt stress. Plant Cell 6: 251-264

Yang J, Isabel Ordiz M, Jaworski JG, Beachy RN (2011) Induced accumulation of cuticular waxes enhances drought tolerance in *Arabidopsis* by changes in development of stomata. Plant Physiol Biochem 49:1448-1455

Yeats TH, Rose JK (2013) The formation and function of plant cuticles. Plant Physiol 163:5-20

Zhang JY, Broeckling CD, Blancaflor EB, Sledge MK, Sumner LW, Wang ZY (2005) Overexpression of WXP1, a putative *Medicago truncatula* AP2 domain-containing transcription factor gene, increases cuticular wax accumulation and enhances drought tolerance in transgenic alfalfa (*Medicago sativa*). Plant J 42:689-707

Zhang JY, Broeckling CD, Sumner LW, Wang ZY (2007) Heterologous expression of two *Medicago truncatula* putative ERF transcription factor genes, *WXP1* and *WXP2*, in *Arabidopsis* led to increased leaf wax accumulation and improved drought tolerance, but differential response in freezing tolerance. Plant Mol Biol 64:265-278

Zhang Z, Wang W, Li W (2013) Genetic interactions underlying the biosynthesis and inhibition of β-diketones in wheat and their impact on glaucousness and cuticle permeability. PLoS One 8:e54129.

Figure Legends

Figure 1. Phylogenetic analysis of ERF TFs. (A) The tree consists of 130 protein sequences, including five derived from cloned *TaWXPL* genes in this study, eight homologs from other species, 11 wheat ERF sequences retrieved from NCBI and 106 wheat ERF sequences from the PlantTFDB database (http://planttfdb.cbi.pku.edu.cn). Sequences were aligned by ClustalW and a bootstrap consensus tree was generated using the Neighbour-Joining method in MEGA6 (Tamura et al. 2013). The branch with protein sequences (indicated by dots) derived from cloned genes is highlighted in cyan. (B) Multiple sequence alignment (Gille et al. 2014) of 14 selected sequences (contained in the branch highlighted in cyan lines in panel (A) illustrating the conserved AD-WXPL domain. The black box indicates the boundaries of this domain, and the positions of conserved negatively (red) and positively (cyan) charged residues. Secondary structure elements (line: disordered region, α-helix: red/grey) are shown below the sequences.

Figure 2. Expression profiles of *TaWXPL1D* and *TaWXPL2B* in wheat tissues (cultivar Chinese Spring) revealed by Q-PCR. DAP - days after pollination; germ. - germinating. Error bars indicate the standard error of three biological replicates.

Figure 3. Expression of wheat *WXPL* genes in rapidly dehydrating flag leaves of two wheat genotypes, Kukri and RAC875, with contrasting drought tolerance. Expression of *TaWXPL1D* and *TaWXPL2B* was studied by Q-PCR. (A) Appearance of flag leaves, peduncles and spikes of Kukri and RAC875 plants. (B) Expression of wheat *WXPL* genes in rapidly dehydrating flag leaves. Flag leaf samples were sampled at awn emergence. Dehydration was performed using detached flag leaves incubated at ambient temperature for 0, 2, 4 and 7 hours (h). Two-way ANOVA (a source of variation: genotype and time) with the Bonferroni test (P=0.05; F=distribution probability values for genotype and time are <0.05 for both genes) was conducted using GenStat. Error bars indicate the standard errors of three biological replicates. Mean values with the same letters are not significantly different at P<0.05.

Figure 4. Expression of wheat *WXPL* genes under cyclic drought in flag leaves of two wheat genotypes, Kukri and RAC875, with contrasting drought tolerance. Expression of *TaWXPL1D* and *TaWXPL2B* was studied by Q-PCR. Expression of genes was examined at the same time points, after 5, 9, 14, 23 and 25 days (d), using either well-watered (WW) or cyclic drought-exposed (DR) plants. Three cycles of drought were applied at 0, 15 and 24 days; times of watering and two re-watering events are indicated with arrows. Two-way ANOVA (a source of variation: treatment and time) with

the Bonferroni test (P=0.05; F=distribution probability values for treatment and time are 0.353, 0.217, <0.001 and 0.817 for *TaWXPL1D* in Kukri and RAC875, and for *TaWXPL2B* in Kukri and RAC875, respectively) was conducted using GenStat. Error bars indicate the standard errors of three biological replicates. Mean values with the same letters are not significantly different at P<0.05.

Figure 5. Analysis of activation (A) and DNA-binding (B) properties of the TaWXPL1D and TaWXPL2B proteins. (A) Transcriptional activation assays and the localisation of activation domains of wheat WXPL proteins. The assay was performed in yeast using full-length and N- or C-terminal truncated WXPL TFs fused to a binding domain (BD) of yeast GAL4 TF. An empty pGBKT7 plasmid was used as a negative control. -Trp represents SD medium lacking tryptophan (selection for plasmid presence) and -Trp/-His, 5mM 3AT refers to the SD medium without tryptophan and histidine but containing 5mM 3-amino-1,2,4-triazole (3AT) (selection for activation of the yeast *HIS3* gene). Domain structures and positions of truncations are indicated in the right part of Fig. 5A. AP2 - APETALA 2 DNA binding domain. D1, D2 and D3 represent removed protein fragments; the residue positions of truncation positions are indicated. (B) DNA-binding selectivity of wheat WXPL proteins shown in the Y1H assay. Each of the constructs expressing recombinant AD-WXPL proteins was transformed into each of four yeast strains (based on Y187) with integrated tandem repeats of DRE, CRT, GCC-box and HDZ1 *cis*-elements upstream of a minimal promoter of the reporter gene. Yeast transformants carrying the plasmids were selected on synthetic defined (SD) (-Leu) medium and replica-plated to SD2 (-Leu, -His, 10mM 3AT) medium. The ability of transformants to grow on SD2 medium suggested an interaction of wheat WXPL proteins with corresponding *cis*-elements.

Figure 6. Molecular features of wheat WXPL proteins in complex with DNA *cis*-elements. (A) The sequence alignment of AP2 domains of TaWXPL1D, TaWXPL2B and AtERF1. Identical residues between the template and target sequences are coloured; colouring based on the properties of the amino acid residues. Secondary structure elements are indicated above the sequences (C: coil, S: sheet, H: α-helix). Boxed residues indicate the positions of residues that form interactions with DNA *cis*-elements. (B) Ribbon representations show the disposition of secondary structures, where antiparallel strands carry the residues that contact DNA *cis*-elements. Structural models of TaWXPL1D and TaWXPL2B are coloured in green and cyan, respectively. The antisense strands of CRT 5′-GTCGGC-3′, DRE 5′-GTCGGT-3′, and GCC 5′-GGCGGC-3′ *cis*-elements are shown in sticks, whereby the sixth bases ($C_{6'}$ or $T_{6'}$) are coloured in cpk yellow. The nucleobases at the first

(G_1 or A_1), fourth (G_4) and fifth (A_5) positions of DNA sense strands are shown in sticks, and the first nucleobases are coloured in cpk yellow. Interactions between amino acid residues and DNA *cis*-elements are shown as dashed lines at 2.5 Å to 3.5 Å separations.

Figure 7. Activation of promoters of cuticle-related genes *TaATT1* and *TaKCS1* by wheat WXPL TFs, as revealed by a transient expression assay in a wheat suspension culture. (A) Schematic showing DNA constructs used in the transient expression assay. The reporter *GUS* gene was driven by one of two promoters of cuticle biosynthesis genes, *TaATT1* or *TaKCS1*. In effector constructs, wheat *WXPL* genes were cloned under the control of the ubiquitin promoter. *GFP* served as a negative control. (B) Activation of *GUS* expression fused with promoters of *TaATT1* and *TaKCS1* by WXPL factors. Each reporter construct was co-bombarded with each effector and *GFP* construct into a wheat suspension culture. Student's t-test was performed for significant analysis of data. *, $P<0.05$; **, $P<0.01$. Error bars indicate the standard error of three replicates.

Scheme 1. The proposed roles of TaWXPL1D and TaWXPL2B TFs in regulation of cuticle biosynthesis during wheat response to drought. This scheme is a modification of a previously published scheme described in Bi et al. (2016).

Legends to Supporting Figures

Supporting Figure 1. Schematic diagram of the cyclic drought experiment (modified from Harris et al., 2016). As indicated by stars, plants were watered at three time points. The soil water content gradually decreased after watering until wilting point, at which water was re-applied. Leaf samples for RNA extraction were collected at 5, 9, 14, 23 and 25 days after an initial withholding of water, as indicated by triangles**.**

Supporting Figure 2. Multiple sequence alignment of wheat WXPL proteins from MtWXP1 and MtWXP2 clades suggests the presence of products of three homologous genes: the first group comprises homeologues of the *TaWXPL1* gene, the second group comprises homeologues of the *TaWXPL2* gene, while the remainder of the sequences are protein products of the third, yet uncharacterised *WXPL* gene. APETALA2 (AP2) domain and C-terminal activation domain are underlined.

(A)

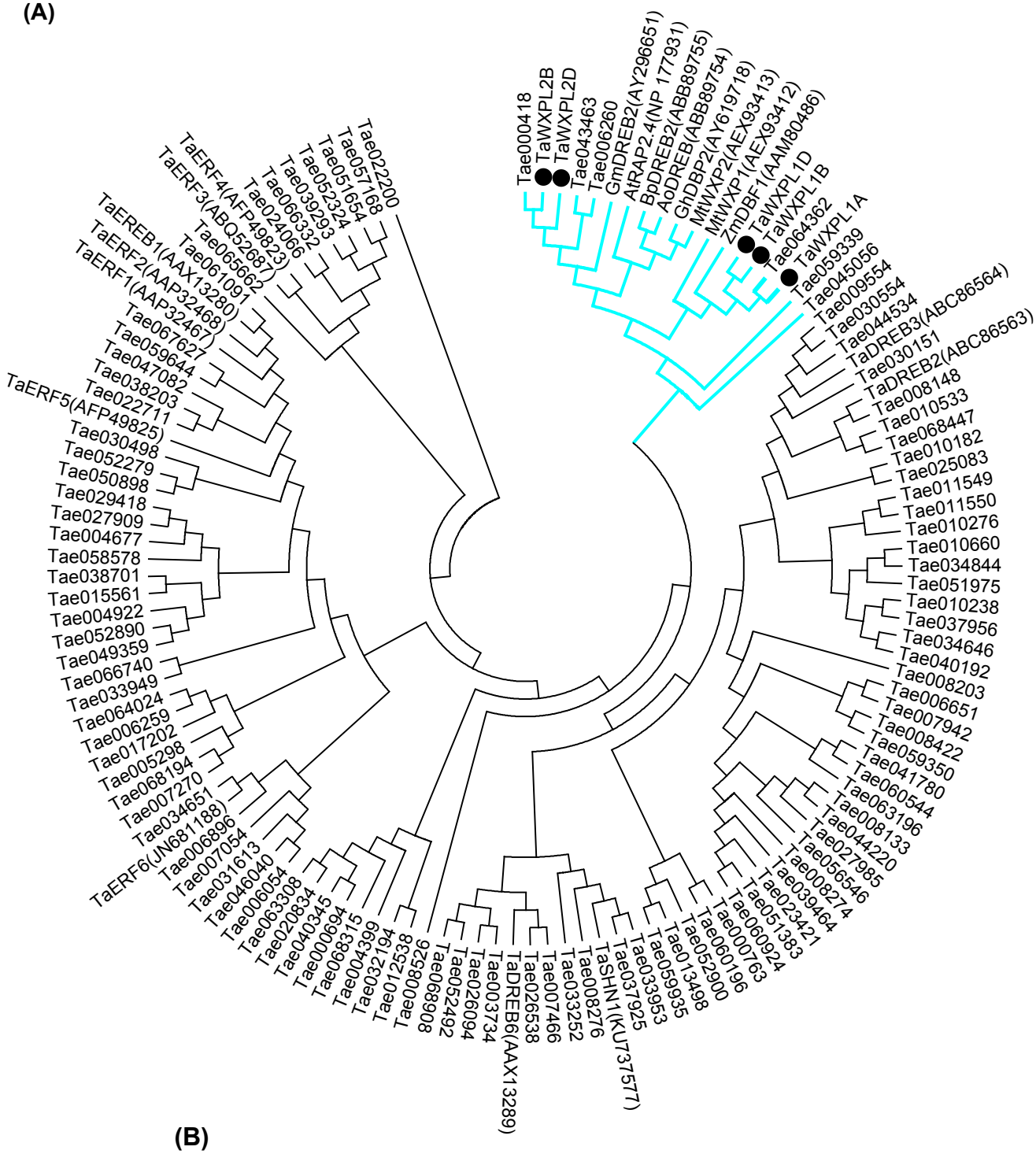
Tae000418
TaWXPL2B
TaWXPL2D
Tae043463
Tae006260
GmDREB2(AY296651)
AtRAP2.4(NP 177931)
BpDREB2(ABB89755)
AoDREB(ABB89754)
GhDBP2(AY619718)
MtWXP2(AEX93413)
MtWXP1(AEX93412)
ZmDBF1(AAM80486)
TaWXPL1D
TaWXPL1B
TaWXPL1A
Tae064362
Tae059339
Tae045056
Tae009554
Tae030554
Tae044534
TaDREB3(ABC86564)
TaDREB2(ABC86563)
Tae030151
Tae008148
Tae010533
Tae068447
Tae010182
Tae025083
Tae011549
Tae011550
Tae010276
Tae010660
Tae034844
Tae051975
Tae010238
Tae037956
Tae034646
Tae040192
Tae008203
Tae006651
Tae007942
Tae008422
Tae059350
Tae041780
Tae060544
Tae063196
Tae008133
Tae044220
Tae027985
Tae056546
Tae008274
Tae039464
Tae023421
Tae051383
Tae060924
Tae000763
Tae060196
Tae052900
Tae013498
Tae059935
Tae033953
TaSHN1(KU737577)
Tae037925
Tae008276
Tae033252
Tae007466
Tae026538
TaDREB6(AAX13289)
Tae003734
Tae026094
Tae052492
Tae008526
Tae068908
Tae012538
Tae032194
Tae004399
Tae068315
Tae000694
Tae040345
Tae020834
Tae063308
Tae006054
Tae046040
Tae031613
Tae007054
Tae006896
TaERF6(JN681188)
Tae034651
Tae007270
Tae068194
Tae005298
Tae017202
Tae006259
Tae064024
Tae033949
Tae066740
Tae049359
Tae052890
Tae004922
Tae015561
Tae038701
Tae058578
Tae004677
Tae027909
Tae029418
Tae050898
Tae052279
Tae030498
TaERF5(AFP49825)
Tae022711
Tae038203
Tae047082
Tae059644
Tae067627
TaERF1(AAP32467)
TaERF2(AAP32468)
TaEREB1(AAX13280)
Tae061091
Tae065663
TaERF3(ABQ52687)
TaERF4(AFP49823)
Tae024066
Tae066332
Tae039293
Tae052324
Tae051654
Tae057168
Tae022200

(B)

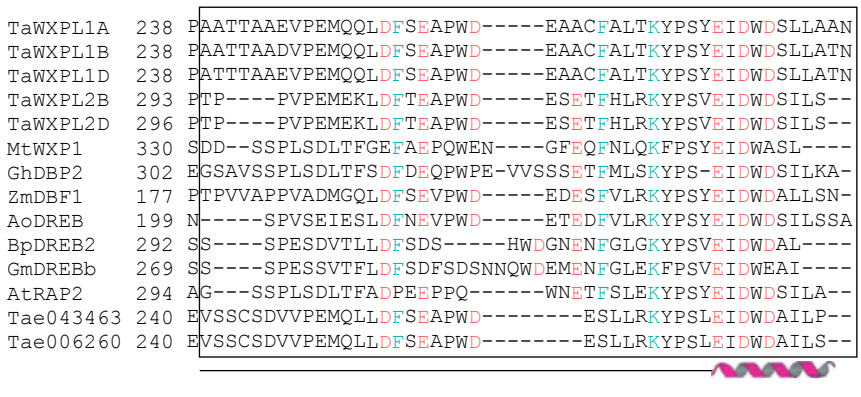
TaWXPL1A 238 PAATTAAEVPEMQQLDFSEAPWD-----EAACFALTKYPSYEIDWDSLLAAN
TaWXPL1B 238 PAATTAADVPEMQQLDFSEAPWD-----EAACFALTKYPSYEIDWDSLLATN
TaWXPL1D 238 PATTTAAEVPEMQQLDFSEAPWD-----EAACFALTKYPSYEIDWDSLLATN
TaWXPL2B 293 PTP----PVPEMEKLDFTEAPWD-----ESETFHLRKYPSVEIDWDSILS--
TaWXPL2D 296 PTP----PVPEMEKLDFTEAPWD-----ESETFHLRKYPSVEIDWDSILS--
MtWXP1 330 SDD--SSPLSDLTFGEFAEPQWEN----GFEQFNLQKFPSYEIDWASL----
GhDBP2 302 EGSAVSSPLSDLTFSDFDEQPWPE-VVSSSETFMLSKYPS-EIDWDSILKA-
ZmDBF1 177 PTPVVAPPVADMGQLDFSEVPWD-----EDESFVLRKYPSYEIDWDALLSN-
AoDREB 199 N-----SPVSEIESLDFNEVPWD-----ETEDFVLRKYPSYEIDWDSILSSA
BpDREB2 292 SS----SPESDVTLLDFSDS-----HWDGNENFGLGKYPSVEIDWDAL----
GmDREBb 269 SS----SPESSVTFLDFSDFSDSNNQWDEMENFGLEKFPSVEIDWEAI----
AtRAP2 294 AG---SSPLSDLTFADPEEPPQ------WNETFSLEKYPSYEIDWDSILA--
Tae043463 240 EVSSCSDVVPEMQLLDFSEAPWD--------ESLLRKYPSLEIDWDAILP--
Tae006260 240 EVSSCSDVVPEMQLLDFSEAPWD--------ESLLRKYPSLEIDWDAILS--

Figure 1

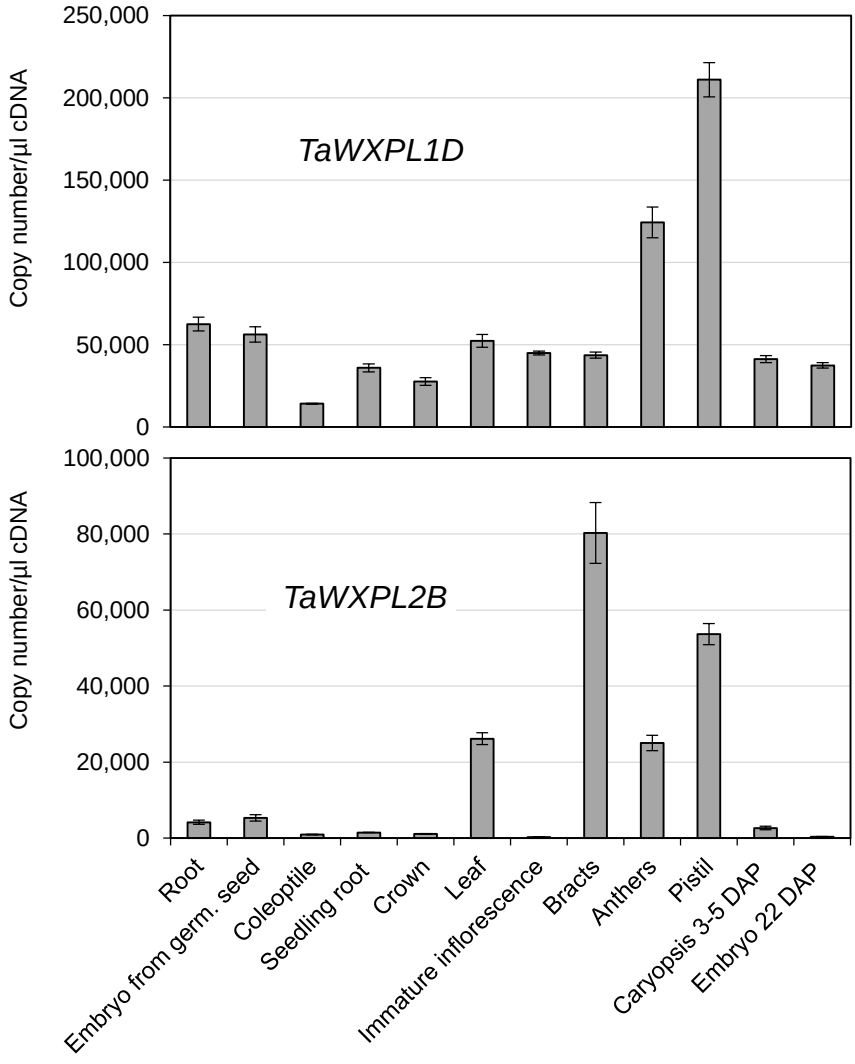
250,000
200,000
150,000
100,000
50,000
0
Copy number/µl cDNA
TaWXPL1D
100,000
80,000
60,000
40,000
20,000
0
Copy number/µl cDNA
TaWXPL2B
Root
Embryo from germ. seed
Coleoptile
Seedling root
Crown
Leaf
Immature inflorescence
Bracts
Anthers
Pistil
Caryopsis 3-5 DAP
Embryo 22 DAP

Figure 2

(A)

Kukri RAC875

(B)

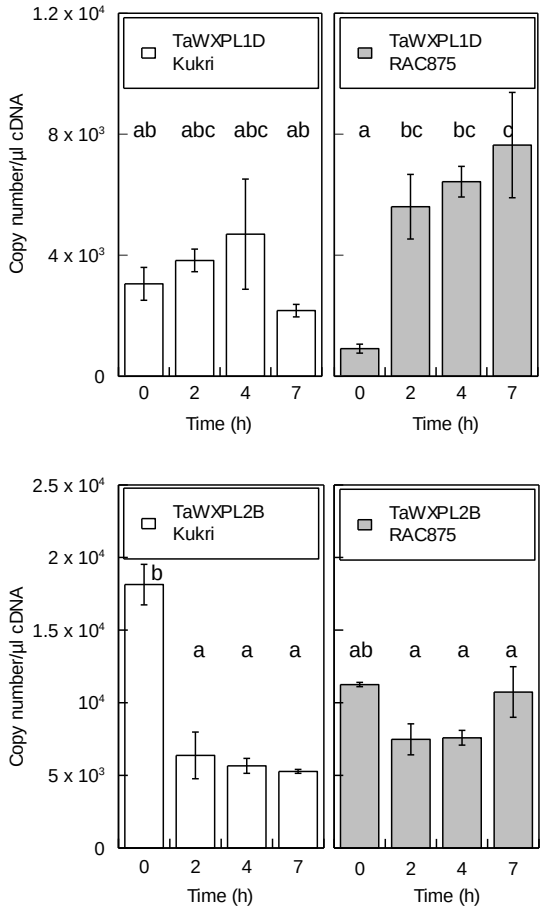

Figure 3

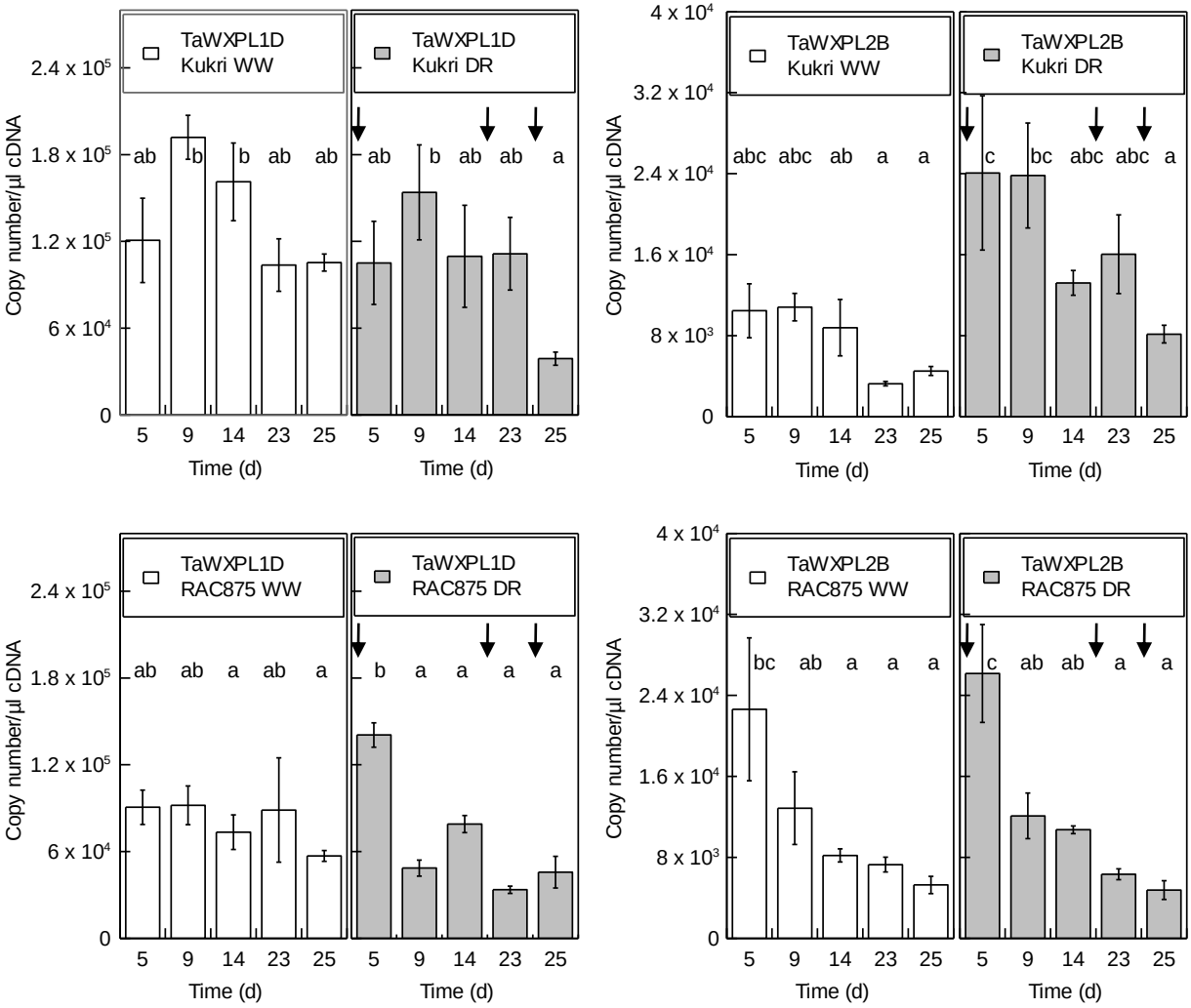
TaWXPL1D
Kukri WW
TaWXPL1D
Kukri DR
TaWXPL2B
Kukri WW
TaWXPL2B
Kukri DR
TaWXPL1D
RAC875 WW
TaWXPL1D
RAC875 DR
TaWXPL2B
RAC875 WW
TaWXPL2B
RAC875 DR
Copy number/µl cDNA
Time (d)
5
9
14
23
25
0
6 x 10⁴
1.2 x 10⁵
1.8 x 10⁵
2.4 x 10⁵
8 x 10³
1.6 x 10⁴
2.4 x 10⁴
3.2 x 10⁴
4 x 10⁴

Figure 4

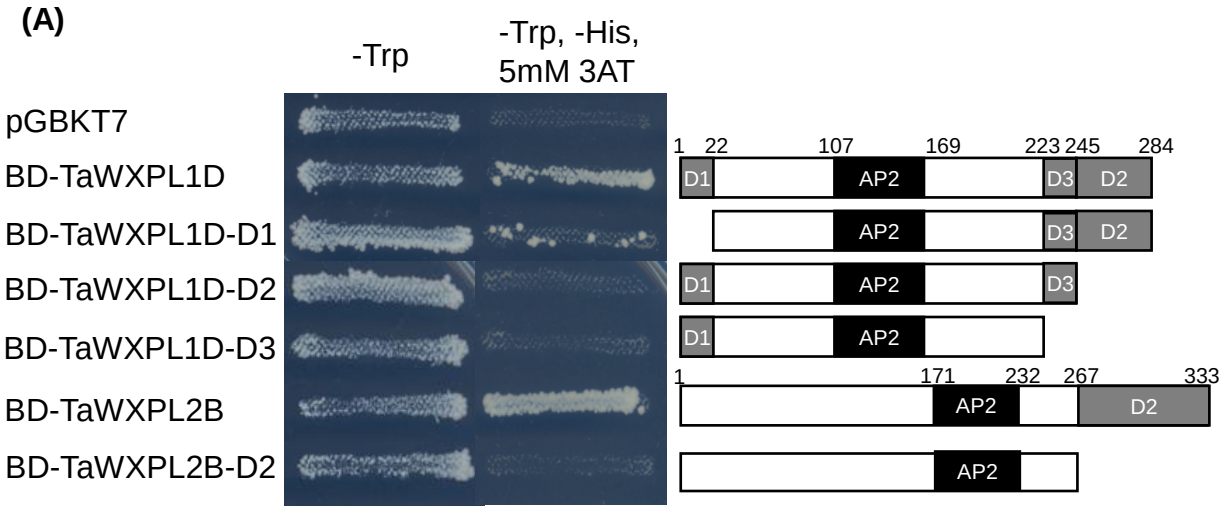
(A)
-Trp
-Trp, -His,
5mM 3AT
pGBKT7
BD-TaWXPL1D
BD-TaWXPL1D-D1
BD-TaWXPL1D-D2
BD-TaWXPL1D-D3
BD-TaWXPL2B
BD-TaWXPL2B-D2
1
22
107
169
223
245
284
D1
AP2
D3
D2
1
171
232
267
333

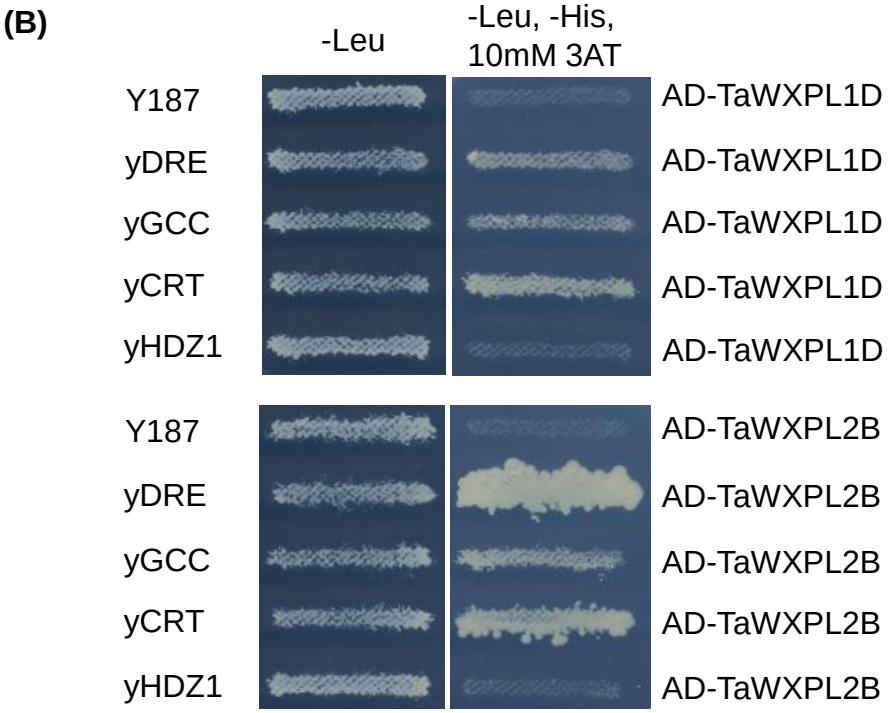
(B)
-Leu
-Leu, -His,
10mM 3AT
Y187
yDRE
yGCC
yCRT
yHDZ1
AD-TaWXPL1D
AD-TaWXPL2B

Figure 5

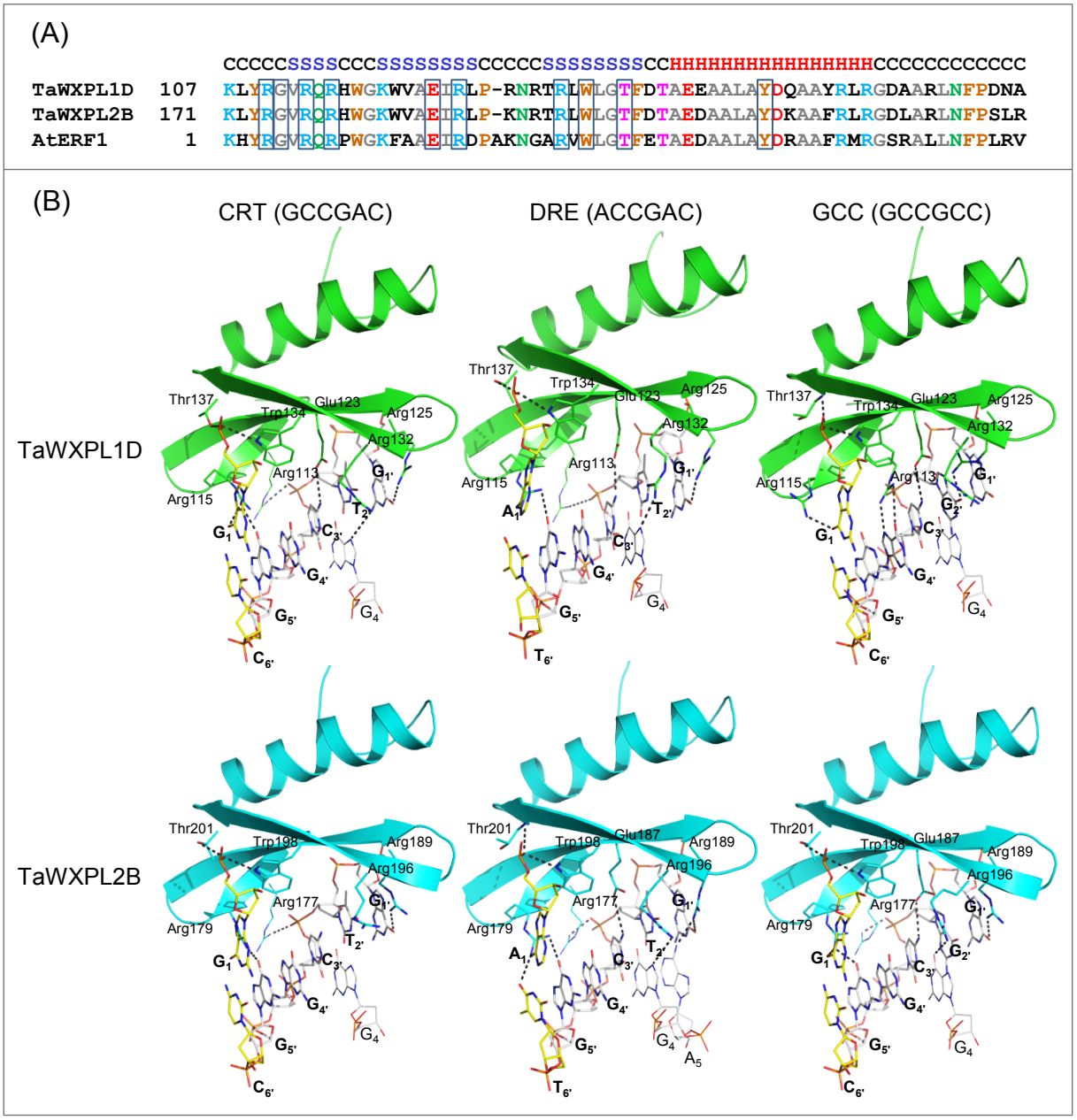
(A)
CCCCCSSSSCCCSSSSSSSSCCCCCSSSSSSSSCCHHHHHHHHHHHHHHHHCCCCCCCCCCCC
TaWXPL1D 107 KLYRGMRQRHWGKWVAEIRLP-RNRTRLWLGTFDTAEEAALAYDQAAYRLRGDAARLNFPDNA
TaWXPL2B 171 KLYRGMRQRHWGKWVAEIRLP-KNRTRLWLGTFDTAEDAALAYDKAAFRLRGDLARLNFPSLR
AtERF1 1 KHYRGMRQRPWGKFAAEIRDPAKNGARVWLGTFETAEDAALAYDRAAFRMRGSRALLNFPLRV
(B)
CRT (GCCGAC)
DRE (ACCGAC)
GCC (GCCGCC)
TaWXPL1D
TaWXPL2B
Thr137
Trp134
Glu123
Arg125
Arg132
Arg113
Arg115
Thr201
Trp198
Glu187
Arg189
Arg196
Arg177
Arg179

Figure 6

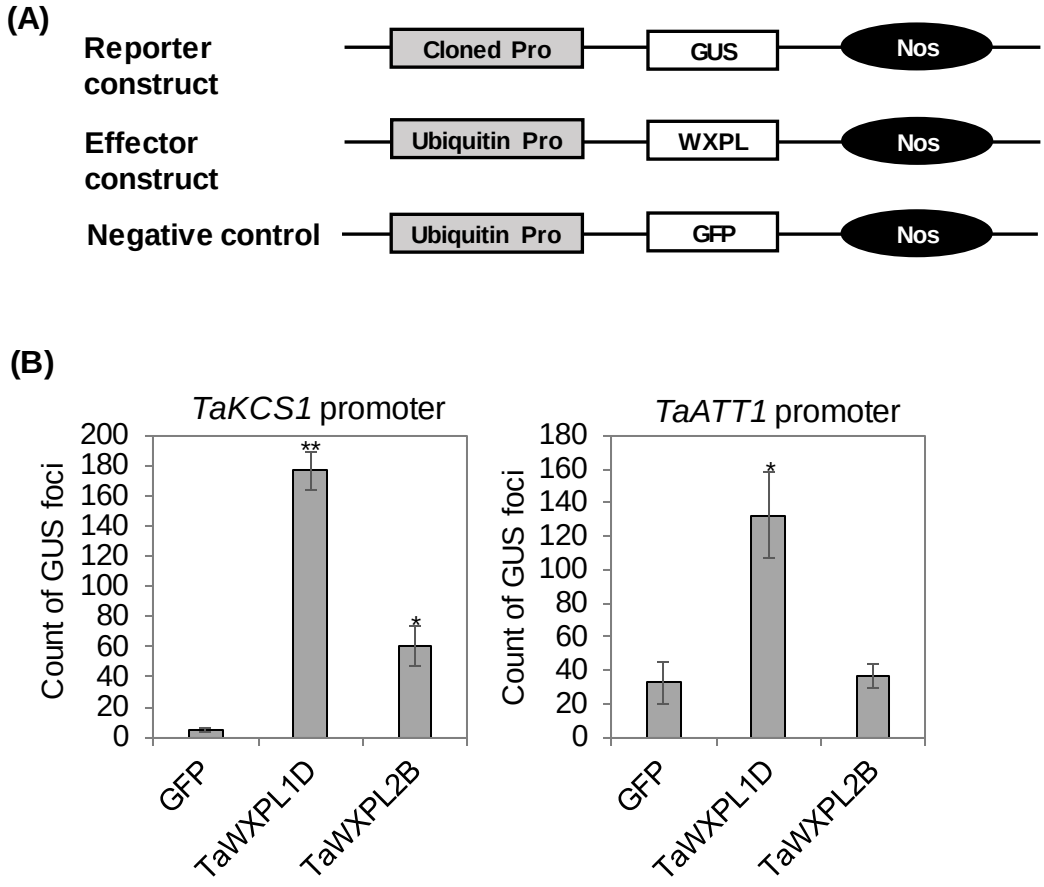
(A)
Reporter construct
Cloned Pro
GUS
Nos
Effector construct
Ubiquitin Pro
WXPL
Nos
Negative control
Ubiquitin Pro
GFP
Nos
(B)
TaKCS1 promoter
Count of GUS foci
200
180
160
140
120
100
80
60
40
20
0
**
*
GFP
TaWXPL1D
TaWXPL2B
TaATT1 promoter
Count of GUS foci
180
160
140
120
100
80
60
40
20
0
*
GFP
TaWXPL1D
TaWXPL2B

Figure 7

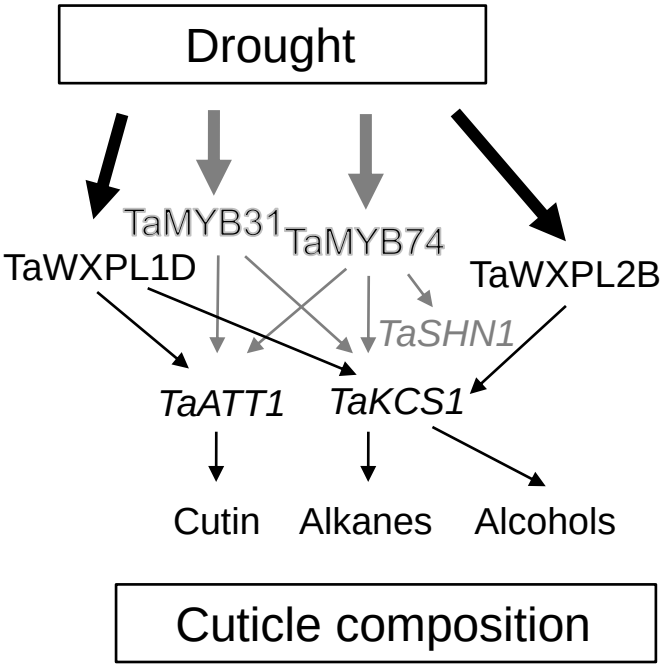
Drought
TaMYB31
TaMYB74
TaWXPL1D
TaWXPL2B
TaSHN1
TaATT1
TaKCS1
Cutin
Alkanes
Alcohols
Cuticle composition

Scheme 1

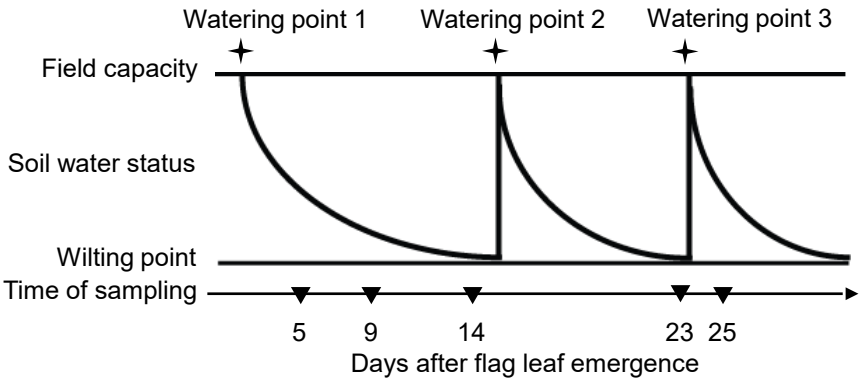

Supporting Figure 1

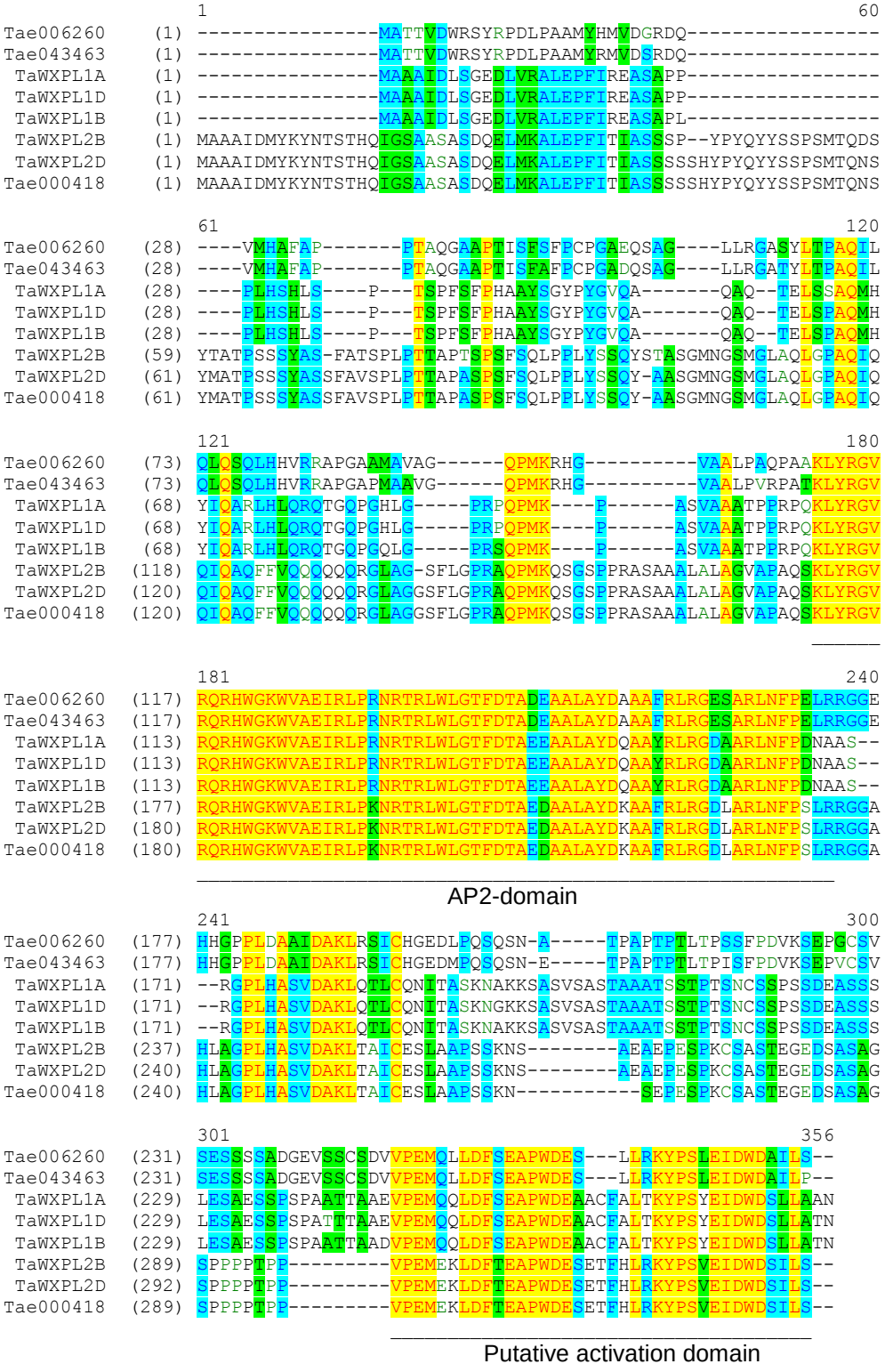

Supporting Figure 2

Supporting Table 1. List of primers used in this study. The directional TOPO cloning overhang (CACC), restriction enzyme sites and protection nucleotides are in bold.

Primer purposes	Genes	Forward primer	Reverse primer
Cloning of *TaWXPL* genes	*TaWXPL1A*	TCCAGGGGCTCCAGATCTGTTCG	GACGGACTAACCAAACCCTACCAC
		CACCATGGCTGCCGCTATAGATCTGTCC	CTAATTGGCGGCGAGAAGCGAGTC
	TaWXPL1B	CCCTATTCGTCTCCTTGTTCACC	GACGGTAGTAATAGTAGCTGACGG
		CACCATGGCTGCAGCTATAGATCTGTCC	CTAATTGGTGGCGAGAAGCGAATC
	TaWXPL1D	CCTGTTCGTCTCCTTGTTCACG	ACGGACTAACCAAACCCTACCCAC
		CACCATGGCTGCCGCTATAGATCTGTCC	CTAATTGGTGGCGAGAAGCGAGTC
	TaWXPL2B	CCCTTGTAGTTCGTCCGAATTATTC	TCTTACTAAACACCACTGGCTAC
		CACCATGGCCGCTGCCATAGACATGTAC	TCACGACAGGATGGAGTCCCAGTC
	TaWXPL2D	CGCTCTCCTCTTGCTCGGGATC	TCTTACTAAACACCACTGGCTAC
		CACCATGGCCGCTGCCATAGACATGTAC	TCACGACAGGATGGAGTCCCAGTC
Gene expression	*TaWXPL1D*	CCTGTTCGTCTCCTTGTTCACG	CGCCTGGCCGATTACTACAG
	TaWXPL2B	GCTATGATGTAATTTCTCTTTCG	CACTGGCTACTTACTGCTAC
Yeast 1-hybrid and in-yeast activation assays	*TaWXPL1D*	**GAAGAATTC**ATGGCTGCCGCTATAGATCTG	**GGAGGATCC**CTAATTGGTGGCGAGAAGC
	TaWXPL1D-D1	**GAAGAATTC**ATGGCCTCTGCCCCCCCTC	**GGAGGATCC**CTAATTGGTGGCGAGAAGC
	TaWXPL1D-D2	**GAAGAATTC**ATGGCTGCCGCTATAGATCTG	**GGAGGATCC**TATGCTGCGGTGGTGGTG
	TaWXPL1D-D3	**GAAGAATTC**ATGGCTGCCGCTATAGATCTG	**GGAGGATCC**TAGGAGGACGGCGAGGAGCAG
	TaWXPL2B	**CATCATATG**GCCGCTGCCATAGAC	**GAAGAATTC**ACGACAGGATGGAGTCC
	TaWXPL2B-D1	**CATCATATG**GCCGCTGCCATAGAC	**GAAGAATTC**AGGCCGAGTTCTTGGACGAG

Supporting Table 2. Evaluation of AP2 TaWXPL structural models in complex with CRT, DRE and GCC *cis*-elements, and the AtERF1 template. Discrete Optimised Protein Energy (DOPE)/Modeller Object Function (MOF) (Modeller 9.16), Ramachandran statistics (allowed residues from PROCHECK), G-factor (from PROCHECK) and z-score (ProSa2003) parameters are given.

Model/DNA complex	DOPE/MOF	Allowed residues	G-factors	z-score
TaWXPL1D/CRT	-4845.91/561.45	100	-0.2	-5.47
TaWXPL1D/DRE	-4842.21/538.62	100	-0.2	-5.44
TaWXPL1D/GCC	-4743.61/527.67	100	-0.1	-5.63
TaWXPL2B/CRT	-4838.09/516.73	100	-0.1	-5.23
TaWXPL2B/DRE	-4857.21/537.41	100	-0.2	-4.82
TaWXPL2B/GCC	-4834.81/522.40	100	-0.1	-5.27
AtERF1	-4916.53/-	100	-0.2	-5.54

Supporting Table 3. Hydrogen bonds of AP2 of TaWXPL1D and TaWXPL2B with CRT (5'-GCCGAC-3'/5'-GTCGGC-3'), DRE (5'-ACCGAC-3'/5'-GTCGGT-3') and GCC (5'-GCCGCC-3'/5'-GGCGGC-3') *cis*-elements.

Residues	**Number of hydrogen bonds with CRT and distances in Å[1]**									**DNA phospho-diester backbone**	**Number**
	CRT										
	G_1	**C_2**	**G_4**	**A_5**	**$G_{1'}$**	**$T_{2'}$**	**$C_{3'}$**	**$G_{5'}$**	**$C_{6'}$**		
TaWXPL1D											
Arg110	-	-	-	-	-	-	-	-	-	1 (2.9)	1
Gly111	-	-	-	-	-	-	-	-	-	1 (2.7)	1
Arg113	-	-	-	-	-	-	-	-	-	1 (2.6)	1
Arg115	1 (2.9)	-	-	-	-	-	-	1 (2.9)	-	-	2
Glu123	-	-	-	-	-	-	1 (3.4)	-	-	-	1
Arg125	-	-	-	-	2 (2.8, 2.9)	-	-	-	-	-	2
Arg132	-	-	1 (3.4)	-	-	-	-	-	-	1 (2.9)	2
Trp134	-	-	-	-	-	-	-	-	-	1 (3.1)	1
Thr137	-	-	-	-	-	-	-	-	-	1 (2.5)	1
Tyr148	-	-	-	-	-	-	-	-	-	1 (2.8)	1
Total	1	0	1	0	2	0	1	1	0	7	13
TaWXPL2B											
Arg174	-	-	-	-	-	-	-	-	-	1 (2.8)	1
Gly175	-	-	-	-	-	-	-	-	-	1 (2.7)	1
Arg177	-	-	-	-	-	-	-	-	-	1 (3.1)	1
Arg179	1 (3.1)	-	-	-	-	-	-	1 (3.0)	-	-	2
Glu187	-	-	-	-	-	-	-	-	-	-	0
Arg189	-	-	-	-	1 (3.0)	-	-	-	-	1 (3.0)	2
Arg196	-	-	-	-	-	-	-	-	-	1 (2.6)	1
Trp198	-	-	-	-	-	-	-	-	-	1 (2.9)	1
Thr201	-	-	-	-	-	-	-	-	-	1 (3.1)	1
Tyr212	-	-	-	-	-	-	-	-	-	1 (2.7)	1
Total	1	0	0	0	1	0	0	1	0	8	11

[1] The separations equal or less than 3.5 Å are indicated in brackets.

Residues	Number of hydrogen bonds with DRE and distances in Å[1]									DNA phospho-diester backbone	Number
	DRE										
	A_1	**C_2**	**G_4**	**A_5**	**$G_{1'}$**	**$T_{2'}$**	**$C_{3'}$**	**$G_{5'}$**	**$T_{6'}$**		
TaWXPL1D											
Arg110	-	-	-	-	-	-	-	-	-	1 (2.9)	1
Gly111	-	-	-	-	-	-	-	-	-	1 (2.7)	1
Arg113	-	-	-	-	-	-	-	-	-	1 (3.4)	1
Arg115	1 (2.5)	1 (3.5)	-	-	-	-	-	1 (2.9)	-	-	3
Glu123	-	-	-	-	-	-	1 (3.3)	-	-	-	1
Arg125	-	-	-	-	1 (2.9)	-	-	-	-	1 (2.9)	2
Arg132	-	-	2 (2.7, 2.8)	-	-	1 (3.1)	-	-	-	-	3
Trp134	-	-	-	-	-	-	-	-	-	1 (2.9)	1
Thr137	-	-	-	-	-	-	-	-	-	1 (3.1)	1
Tyr148	-	-	-	-	-	-	-	-	-	1 (2.7)	1
Total	1	1	2	0	1	1	1	1	0	7	15
TaWXPL2B											
Arg174	-	-	-	-	-	-	-	-	-	1 (2.9)	1
Gly175	-	-	-	-	-	-	-	-	-	1 (2.7)	1
Arg177	-	-	-	-	-	-	-	-	-	1 (2.7)	1
Arg179	1 (2.6)	-	-	-	-	-	-	1 (3.0)	1 (3.3)	-	3
Glu187	-	-	-	-	-	-	1 (3.5)	-	-	-	1
Arg189	-	-	-	1 (2.9)	1 (2.8)	-	-	-	-	-	2
Arg196	-	-	1 (3.3)	-	-	-	-	-	-	1 (2.9)	2
Trp198	-	-	-	-	-	-	-	-	-	1 (3.1)	1
Thr201	-	-	-	-	-	-	-	-	-	1 (3.2)	1
Tyr212	-	-	-	-	-	-	-	-	-	1 (2.5)	1
Total	1	0	1	1	1	0	1	1	1	7	14

[1] The separations equal or less than 3.5 Å are indicated in brackets.

Residues	Number of hydrogen bonds with GCC and distances in Å[1]									DNA phospho-diester backbone	Number
	GCC										
	G_1	**C_2**	**G_4**	**C_5**	**$G_{1'}$**	**$G_{2'}$**	**$C_{3'}$**	**$G_{4'}$**	**$G_{5'}$**		
TaWXPL1D											
Arg110	-	-	-	-	-	-	-	-	-	-	0
Gly111	-	-	-	-	-	-	-	-	-	1 (2.7)	1
Arg113	-	-	-	-	-	-	-	2 (2.9, 3.5)	-	-	2
Arg115	1 (2.6)	-	-	-	-	-	-	-	-	-	1
Glu123	-	-	-	-	-	-	1 (3.5)	-	-	-	1
Arg125	-	-	-	-	1 (2.7)	1 (2.7)	-	-	-	-	2
Arg132	-	-	-	-	-	-	-	-	-	1 (2.9)	1
Trp134	-	-	-	-	-	-	-	-	-	1 (3.1)	1
Thr137	-	-	-	-	-	-	-	-	-	1 (3.1)	1
Tyr148	-	-	-	-	-	-	-	-	-	1 (2.6)	1
Total	1	0	0	0	1	1	1	2	0	5	11
TaWXPL2B											
Arg174	-	-	-	-	-	-	-	-	-	1 (2.9)	1
Gly175	-	-	-	-	-	-	-	-	-	1 (2.7)	1
Arg177	-	-	-	-	-	-	-	-	-	1 (2.9)	1
Arg179	1 (2.3)	-	-	-	-	-	-	-	1 (2.6)	-	2
Glu187	-	-	-	-	-	-	1 (3.4)	-	-	-	1
Arg189	-	-	-	-	1 (3.0)	-	-	-	-	-	1
Arg196	-	-	1 (2.9)	-	-	-	-	-	-	-	1
Trp198	-	-	-	-	-	-	-	-	-	1 (3.1)	1
Thr201	-	-	-	-	-	-	-	-	-	1 (3.1)	1
Tyr212	-	-	-	-	-	-	-	-	-	1 (3.5)	1
Total	1	0	1	0	1	0	1	0	1	6	11

[1] The separations equal or less than 3.5 Å are indicated in brackets.